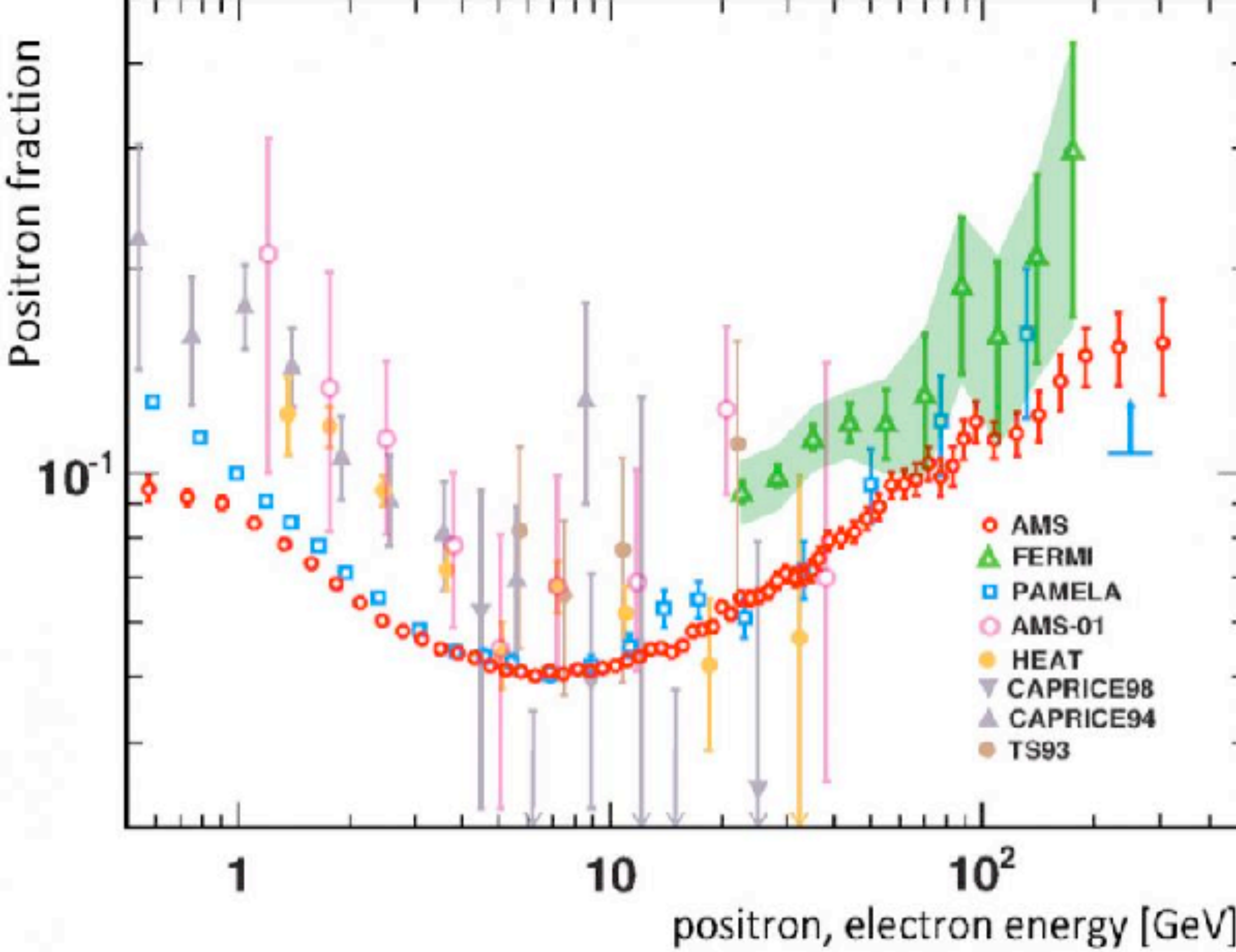

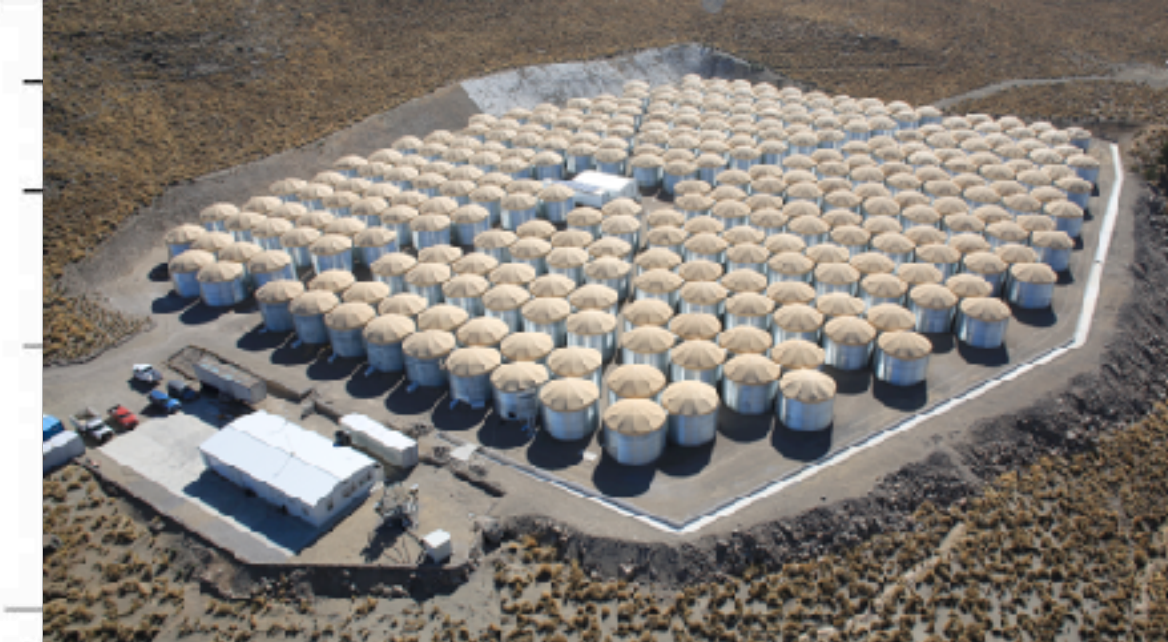

Recent Advances in our Understanding of the Source of the Positron Excess

Tim Linden

CCAPP Postdoctoral Fellow
Center for Cosmology and Astro-Particle Physics
The Ohio State University

CCAPP

THE OHIO STATE UNIVERSITY

Cosmic Rays, Pulsars, and Dark Matter 3/3/17

The Positron Excess

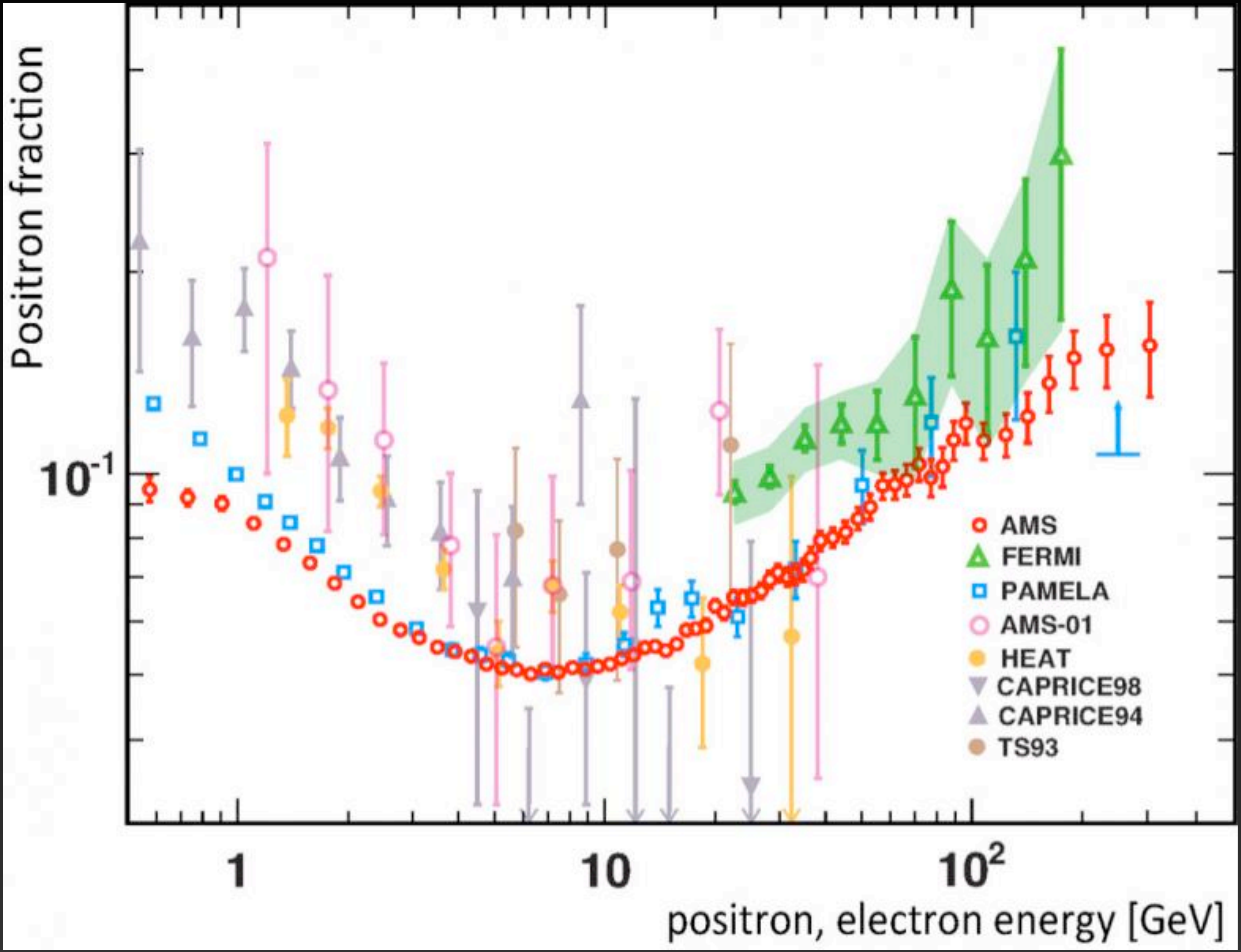

The Positron Excess (Theory)

Cholis & Hooper (2013, 1304.1840)

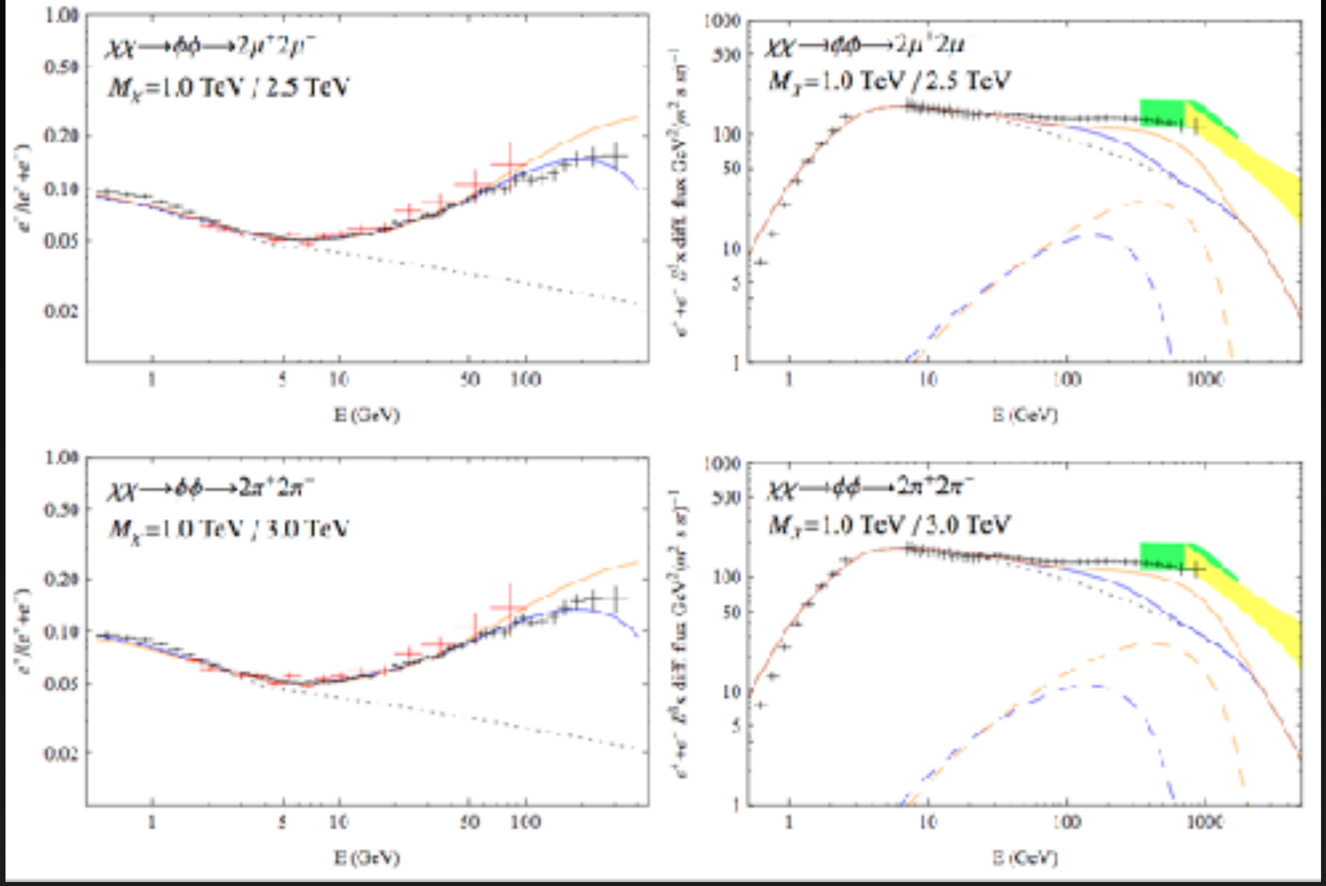

Dark Matter models can explain the rising positron fraction only if the annihilation proceeds through intermediate channels to soften the spectrum.

Lopez et al. (2015, 1501.01618)

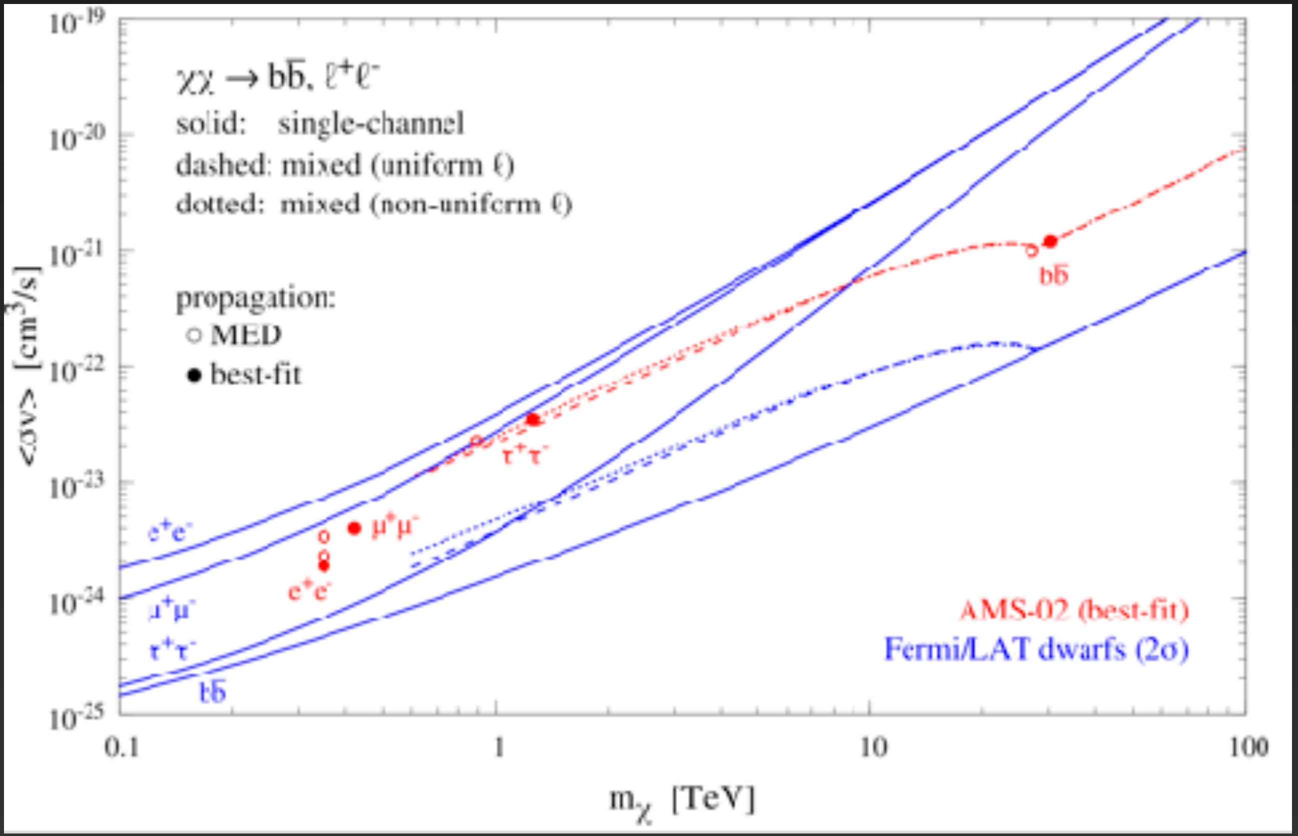

Additionally, Fermi-LAT observations of dwarf spheroidal galaxies strongly constrain most reasonable models.

The Positron Excess (Theory)

Pulsars are also capable of accelerating leptons to PeV energies.

The total spin-down power of pulsars (~10^{50} erg) is capable of powering the observed emission.

Current uncertainties include the supernova rate and the <u>fraction of the pulsar spin-down power that is converted to e^+e^- pairs.</u> (foreshadowing!)

Harding & Ramaty (1987)

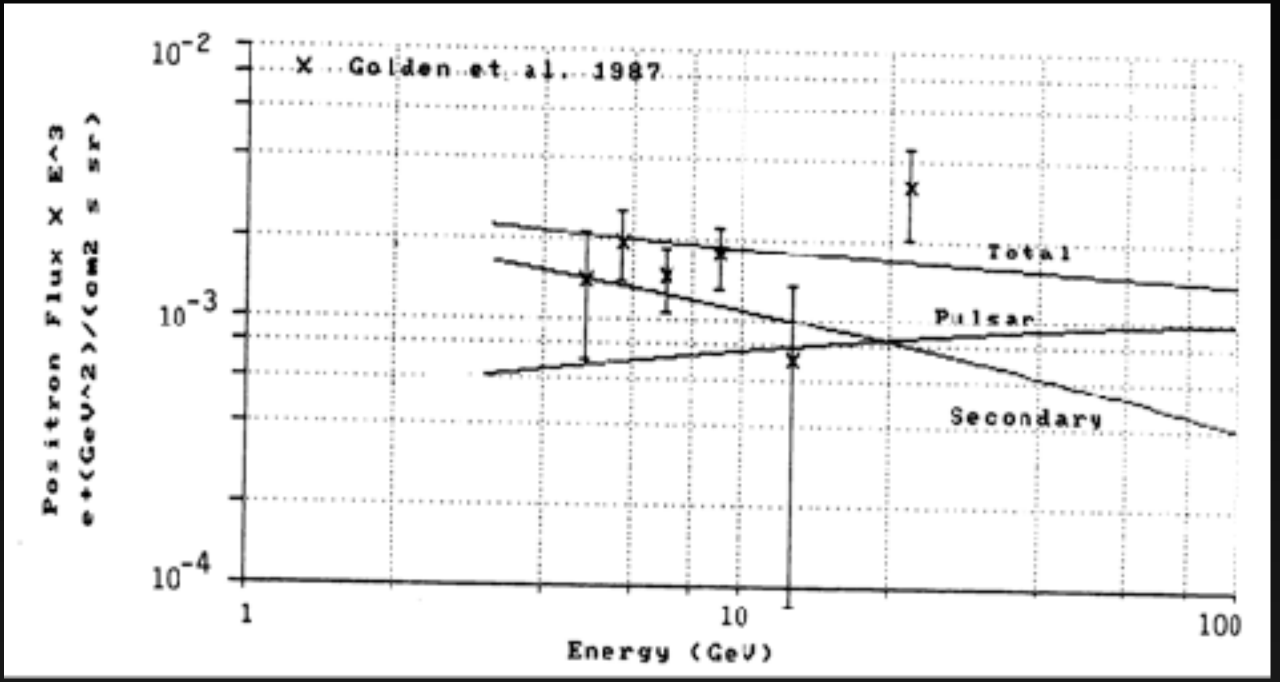

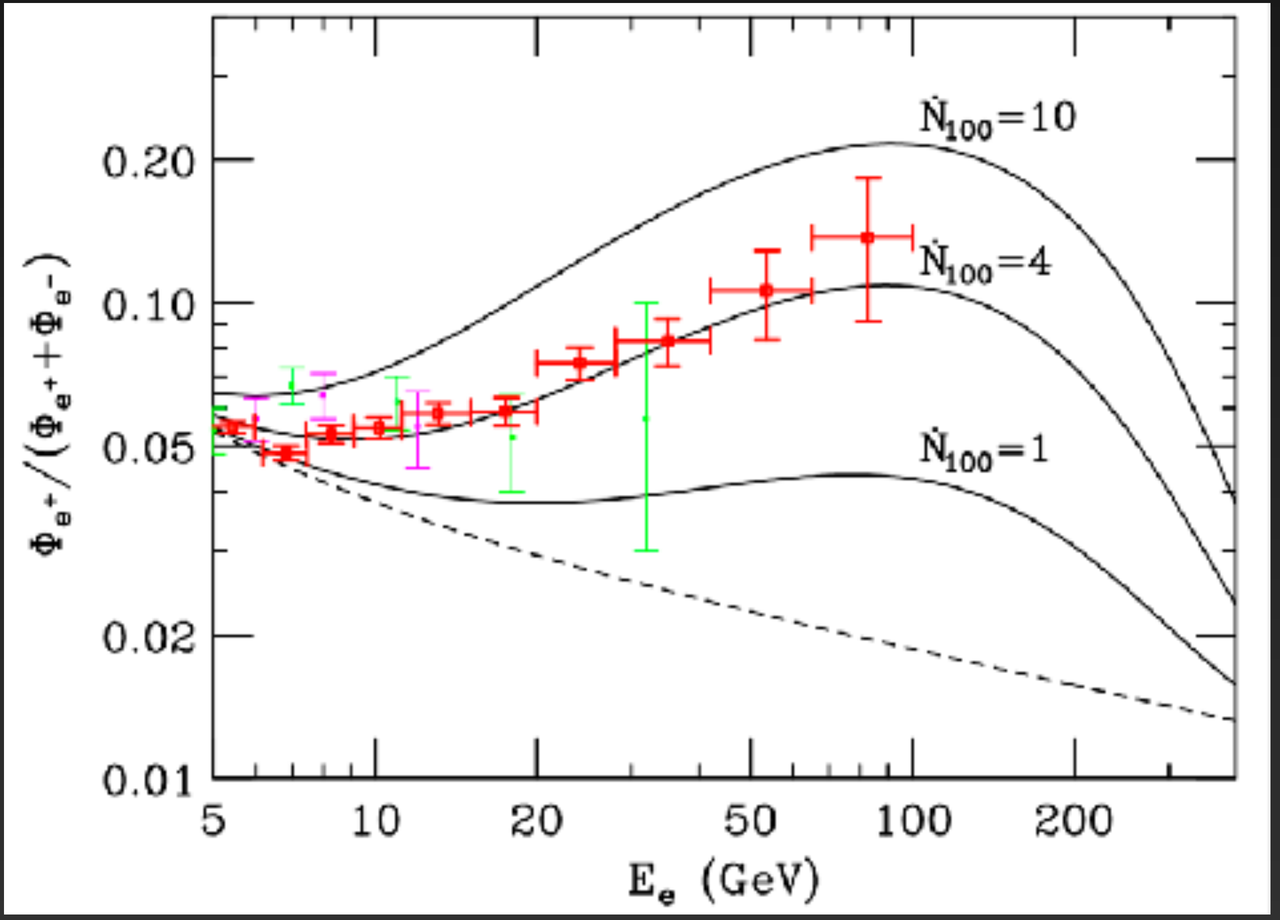

Hooper et al. (2009, 0810.1527)

The Positron Excess (Theory)

The rising positron fraction can also be dominated by a single nearby pulsar.

Prime candidates are Geminga and Monogem.

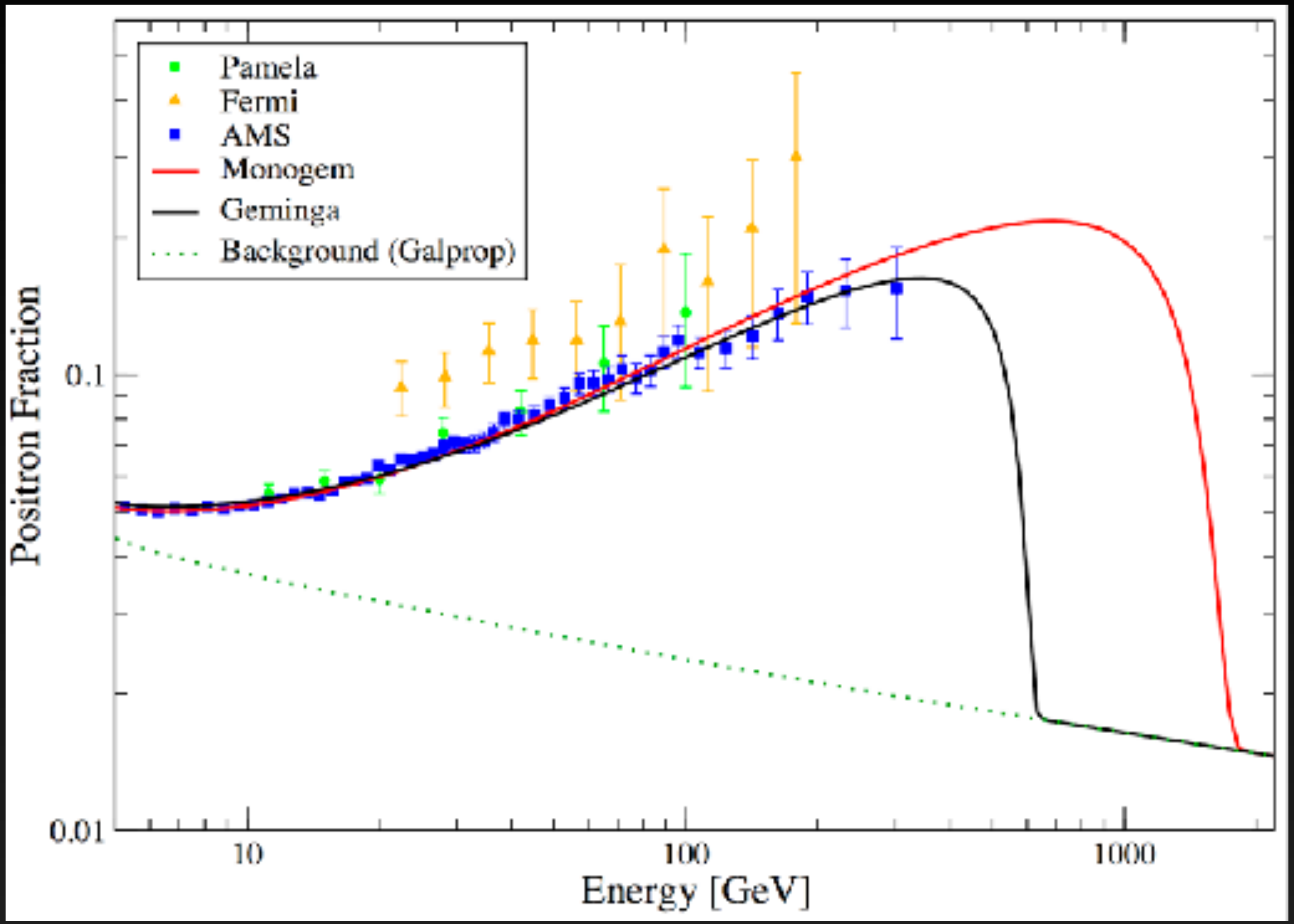

Linden & Profumo (2013, 1304.1791)

This adds some Poisson fluctuations into the determination of the Pulsar contribution. The positron fraction observed at Earth need not be the average positron fraction observed in the Galaxy. (could we constrain this?)

The Positron Excess (Theory)

$$L = \sqrt{6Dt} = \sqrt{6D_0E^{\delta}t}$$

$$\tau_{loss} \propto (\phi_B + \phi_{ISRF})\, E^{-1}$$

$$L_{diff} \propto E^{\delta-1}$$

The reality is likely a combination of the two. Electrons are more contained at high energies, and local pulsars likely dominate the high energy positron flux.

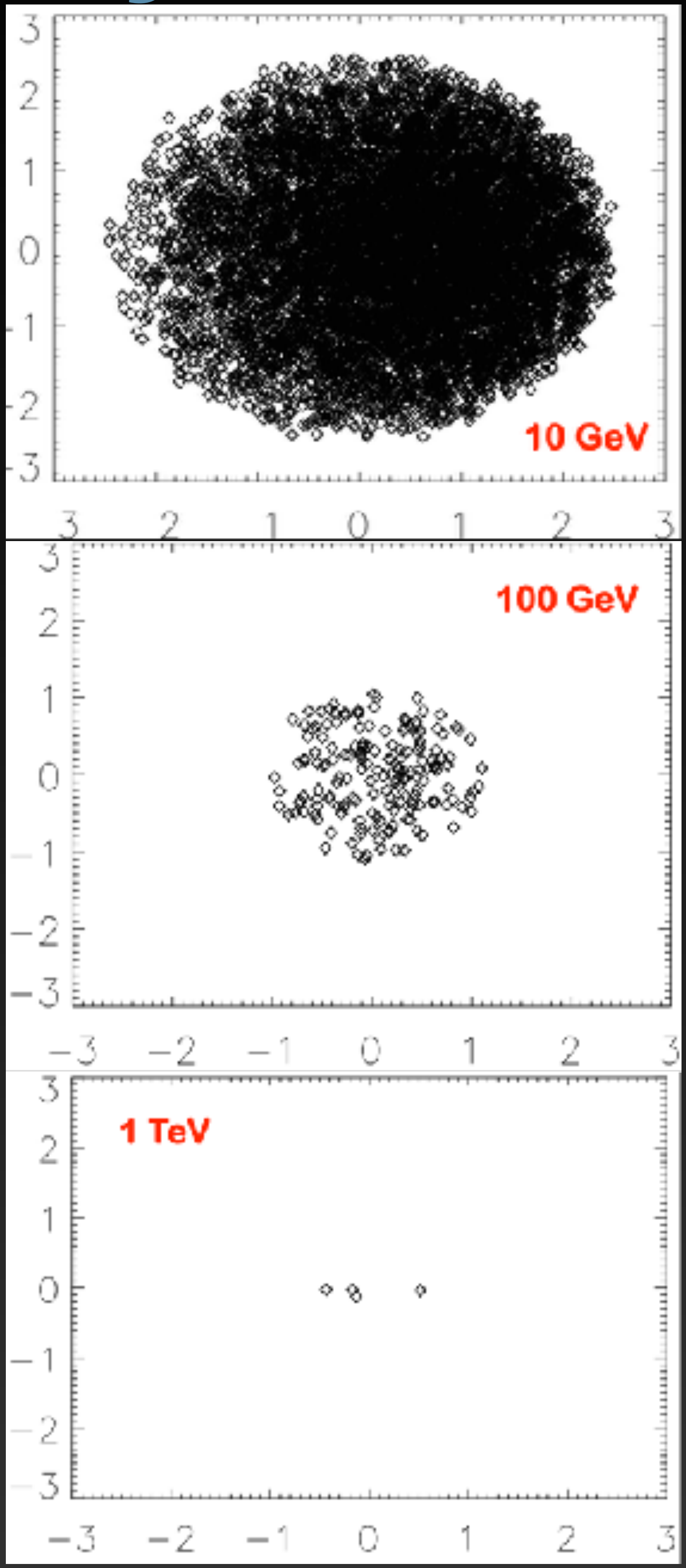

Blasi & Amato (2010, 1007.4745)

The Positron Excess (Theory)

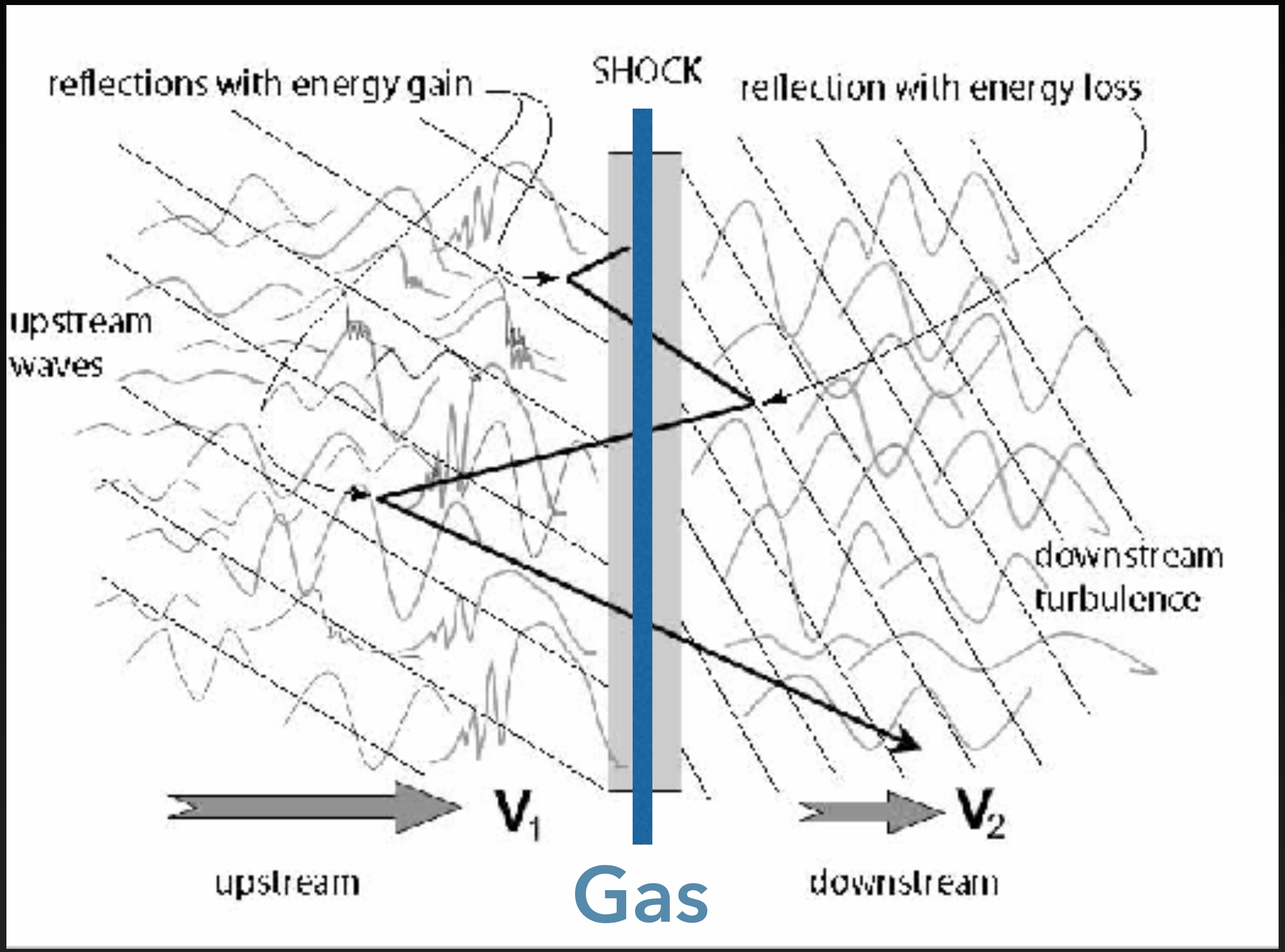

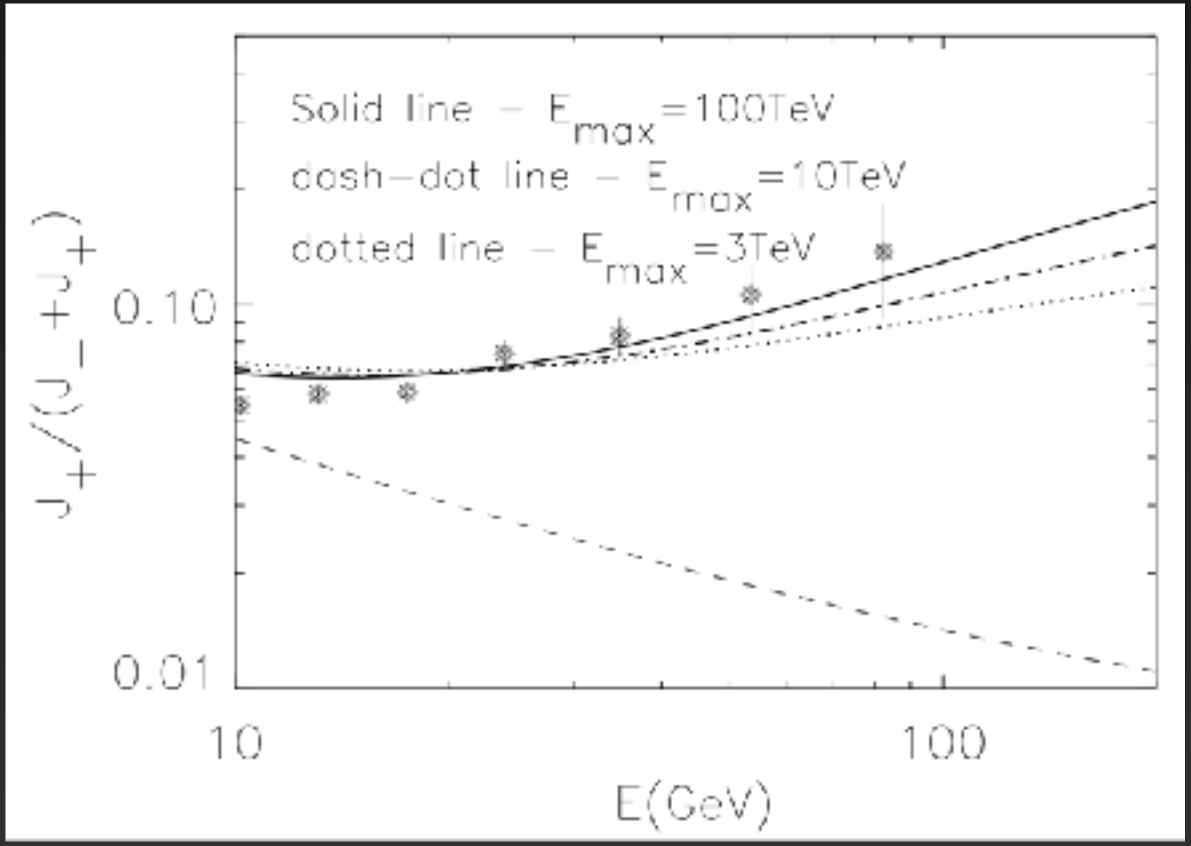

Produce “secondary” particles inside the supernova acceleration region.

Secondaries gain the same spectrum.

Blasi & Amato (2010, 1007.4745)

The Positron Excess (Theory)

How Can We Differentiate these models?

Differentiating Models (Spectrum)

Many have pointed towards a spectral cutoff as a smoking gun of dark matter annihilation.

However, this can also be accommodated in any model with a non-continuous injection morphology.

Note: The pulsar injection spectra on the right are cut off at 2 TeV, the sharp cutoffs in the local positron fraction are due only to cooling.

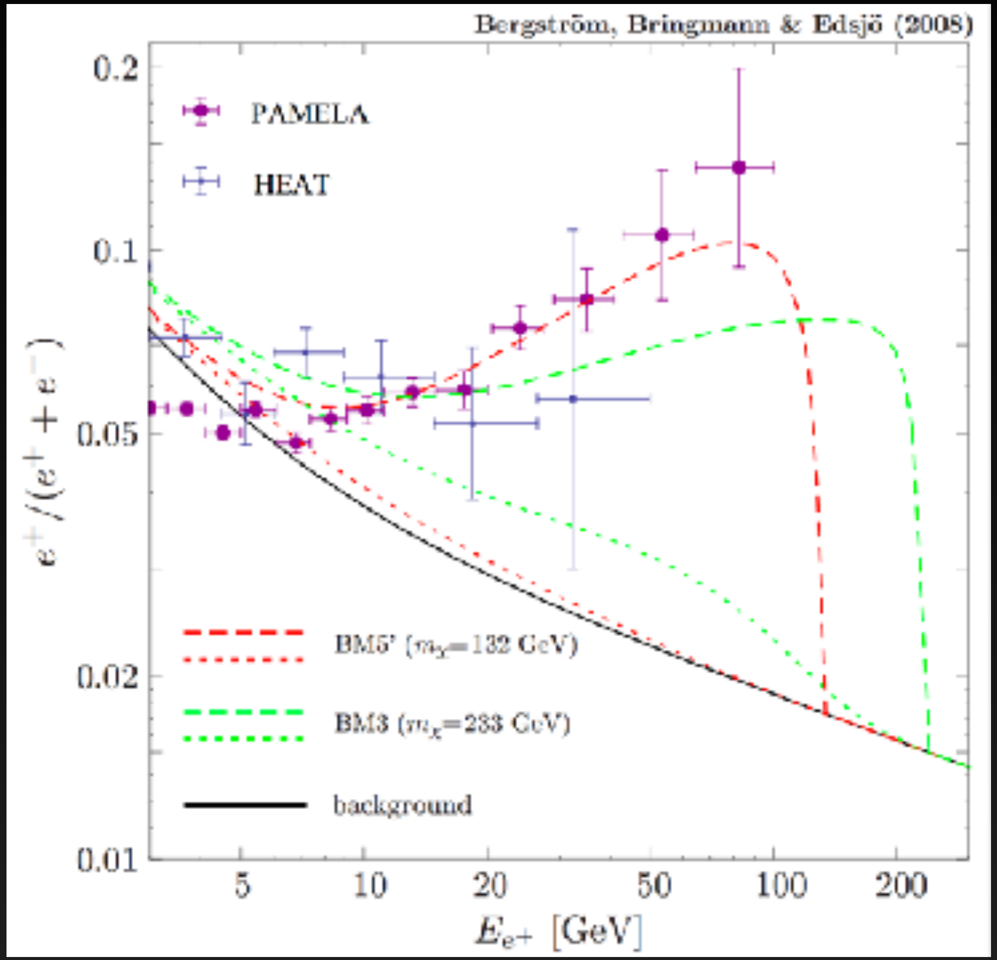

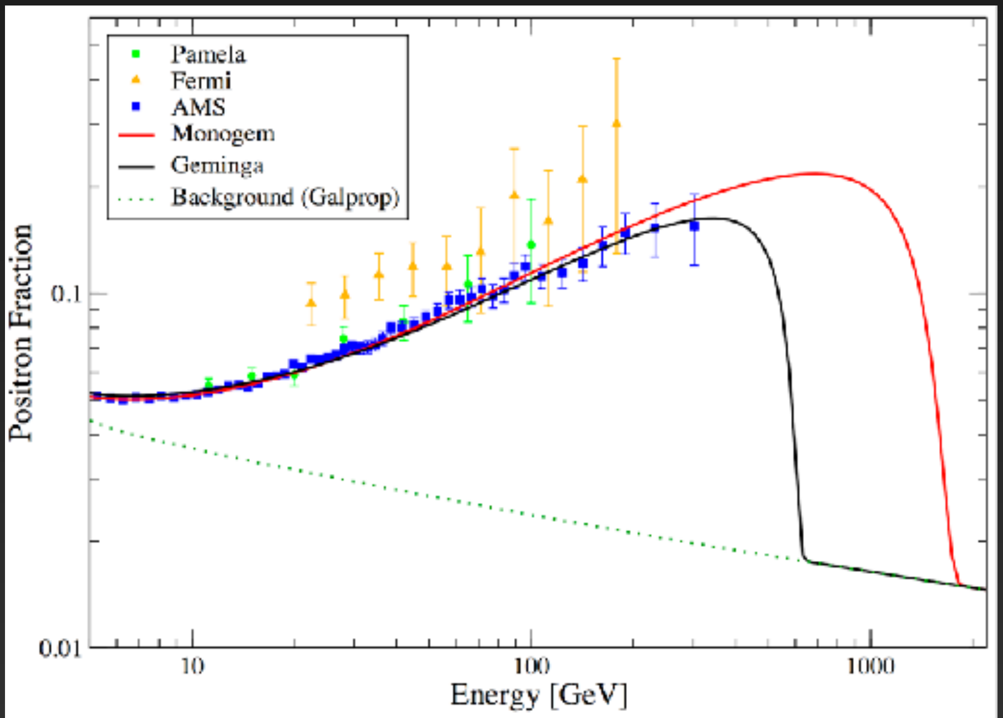

Linden & Profumo (2013, 1304.1791)

Differentiating Models (Wiggles)

Non-Continuous injection sources can produce "wiggles" in the cosmic-ray flux due to Poisson fluctuations from nearby sources.

This is most obvious in leptonic channels due to cooling.

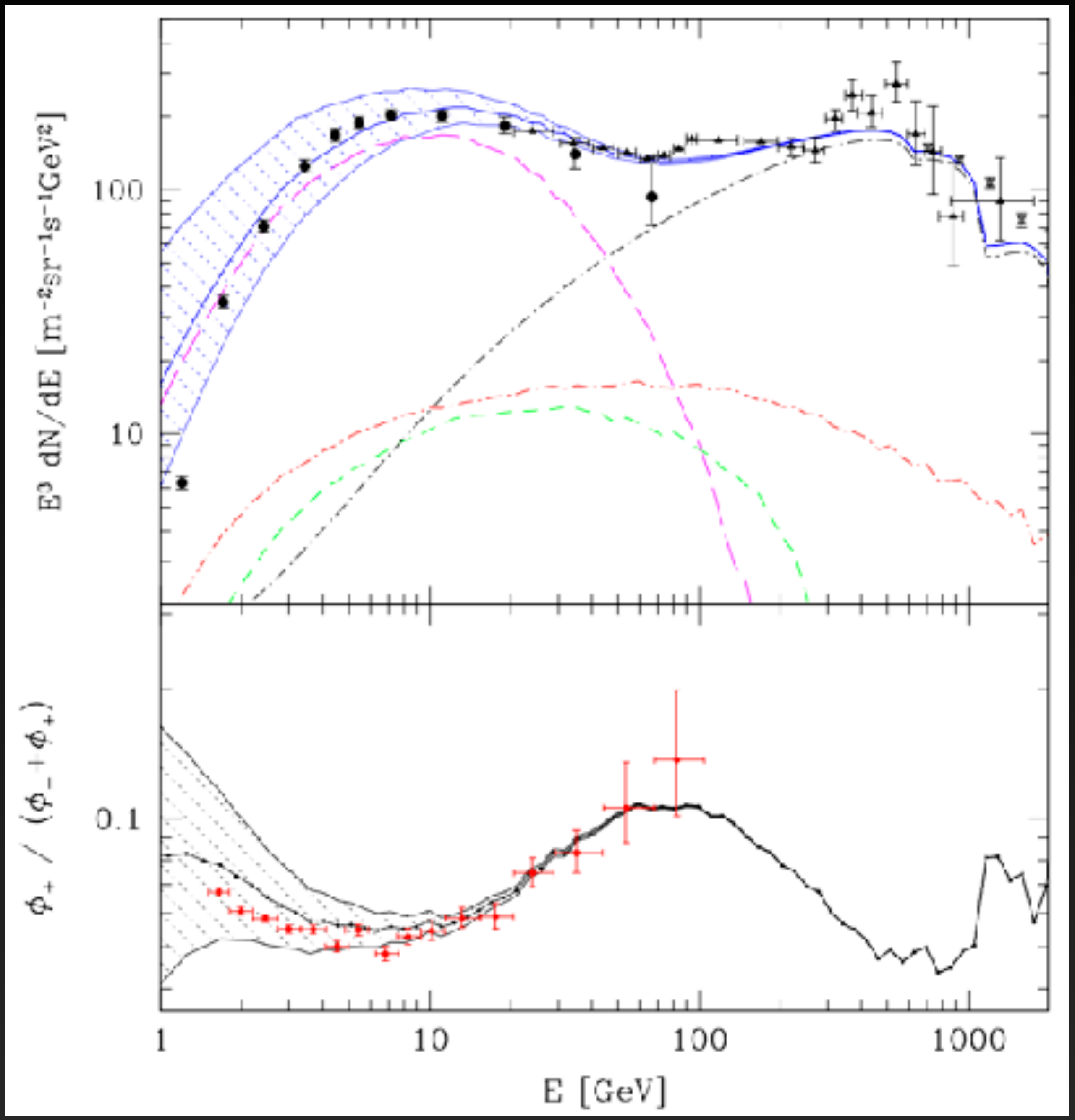

Shaviv et al. (2009, 0902.0376)

Differentiating Models (Secondaries)

Mertsch & Sarkar (2009, 0905.3152)

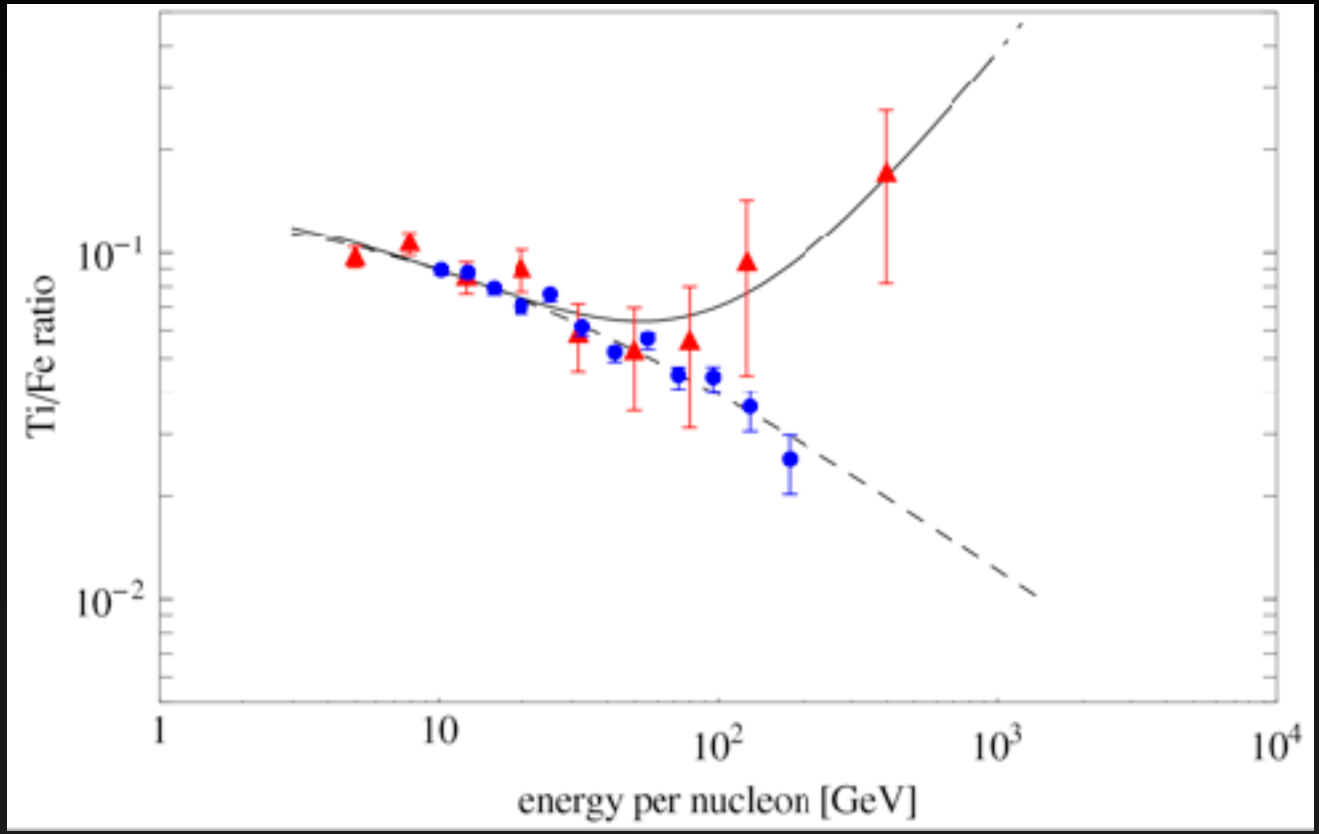

Stochastic acceleration models invariably accelerate all species of secondary particles.

Positrons have the most intense acceleration and are accelerated at the lowest energies. They are the first to be seen.

This scenario may be compatible with Ti/Fe, but may be ruled out by B/C.

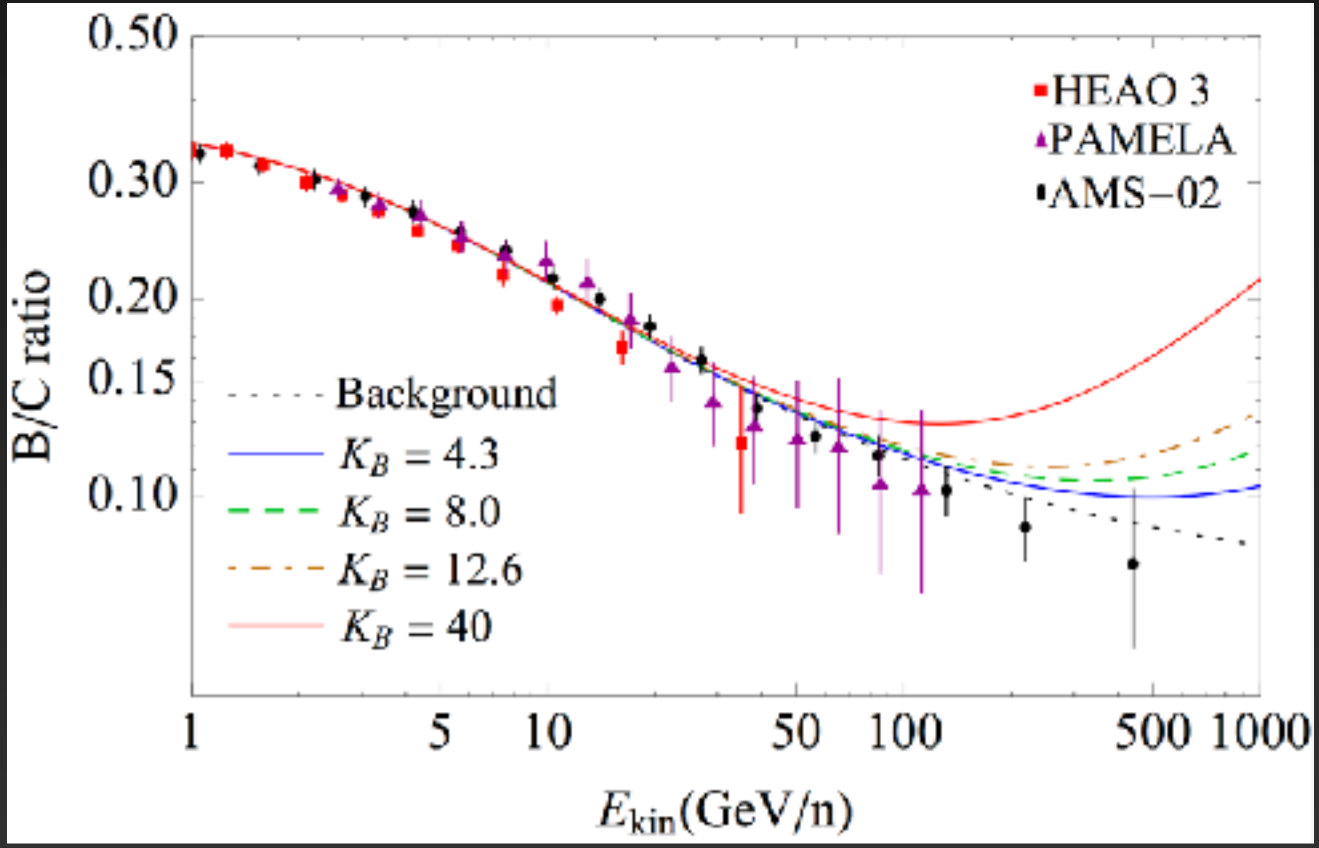

Cholis & Hooper (2013, 1312.2952)

Recent Advances

We will discuss two recent advances in our understanding of astrophysical models for the positron excess:

1.) Stochastic Acceleration

2.) Pulsar Emission

Systematics: Solar Modulation

At low energies. Cosmic rays are significantly affected by the solar wind.

$$\frac{dN^{\oplus}}{dE_{\rm kin}}(E_{\rm kin}) = \frac{(E_{\rm kin}+m)^2 - m^2}{(E_{\rm kin}+m+|Z|e\Phi)^2 - m^2} \times \frac{dN^{\rm ISM}}{dE^{\rm ISM}_{\rm kin}}(E_{\rm kin}+|Z|e\Phi),$$

Typically, models have used the force-field approximation to determine the effect of solar modulation (though see Igor's talk).

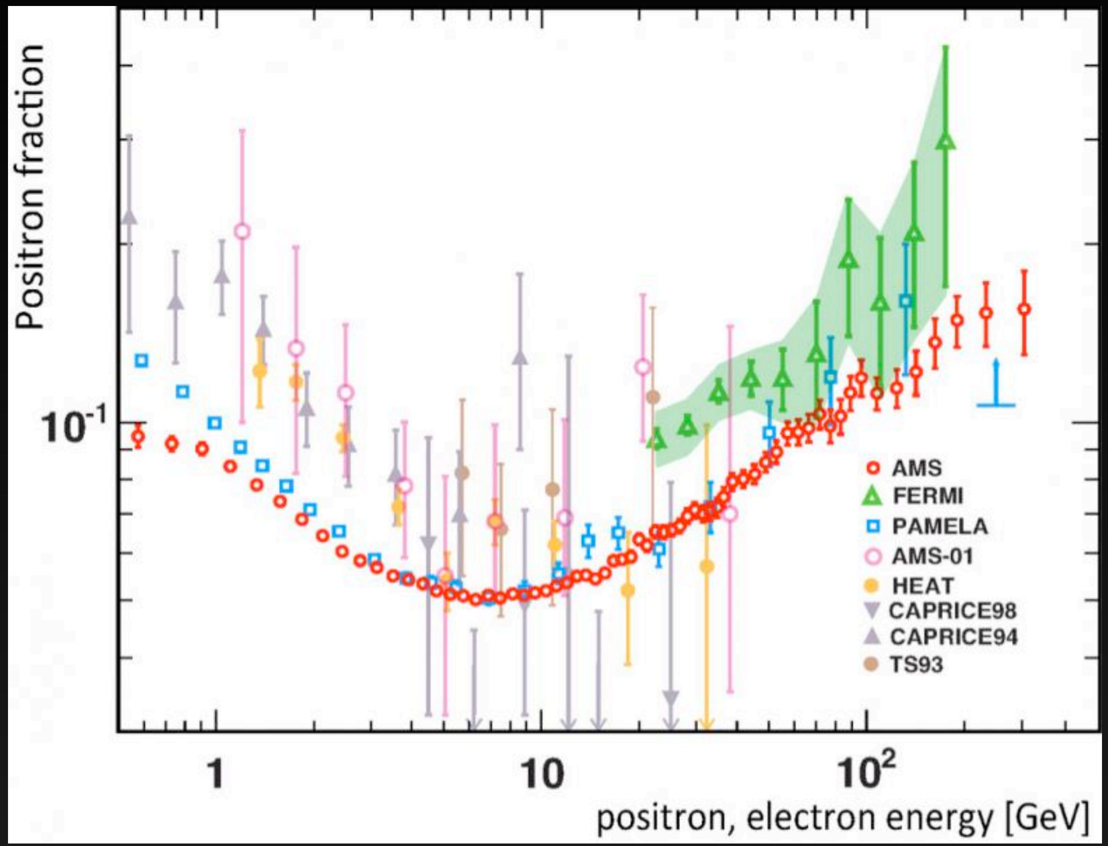

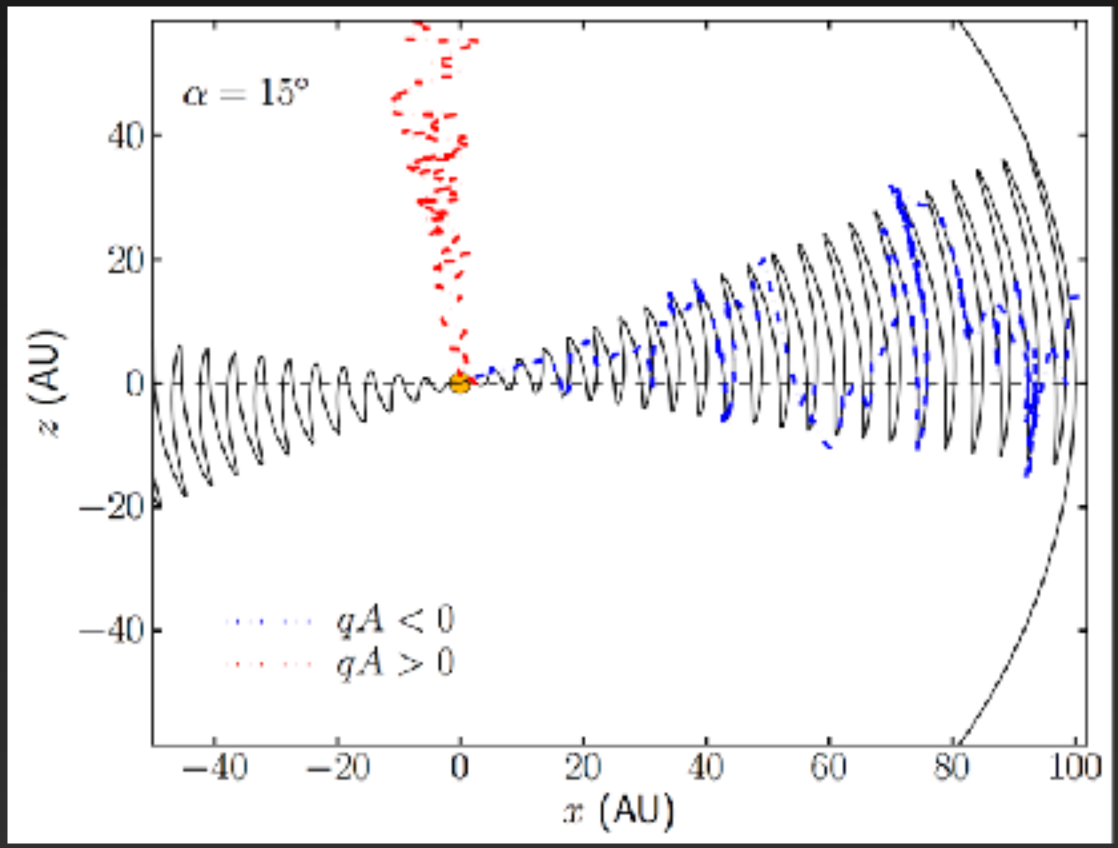

Cholis et al. (2016, 1511.01507)

Solar Modulation

Solar Modulation is dominated by solar activity, and the strength of the solar wind.

These are observable parameters!

$$\Phi(R,t,q) = \phi_0 \left(\frac{|B_{\text{tot}}(t)|}{4\,\text{nT}} \right) + \phi_1\, N'(q) H(-qA(t)) \times \left(\frac{|B_{\text{tot}}(t)|}{4\,\text{nT}} \right) \left(\frac{1 + (R/R_0)^2}{\beta (R/R_0)^3} \right) \left(\frac{\alpha(t)}{\pi/2} \right)^4$$

Era	$\lvert B_{\text{tot}}\rvert$ (nT)	α (degrees)	$N'(q>0) \cdot H(-qA(t))$	$N'(q<0) \cdot H(-qA(t))$
07-12/11	4.7	60.5	1	0
01-06/12	4.8	67.2	1	0
07-12/12	5.3	70.0	0.67	0.33
01-06/13	5.5	71.0	0.50	0.50
07-12/13	5.2	70.0	0.33	0.67
01-06/14	5.3	67.0	0	1
07-12/14	5.6	62.0	0	1
01-06/15	6.6	56.6	0	1

This leads to a predictive solar modulation potential with no degrees of freedom!

Cholis et al. (2016, 1511.01507)

Stochastic Acceleration

Cholis et al. (2017, 1701.04406)

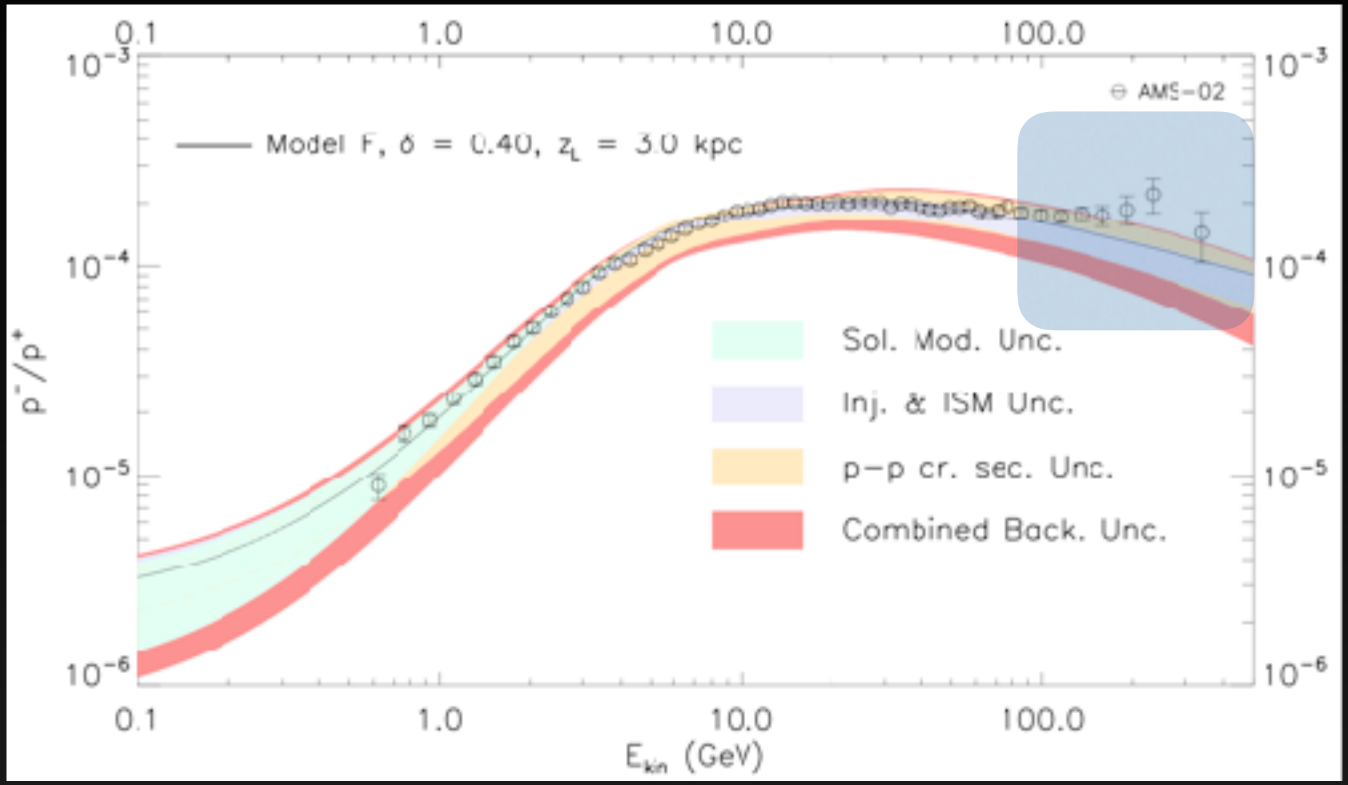

Recent AMS-02 data indicate a hardening of the antiproton ratio at energies above 100 GeV.

This hardening is not expected in any leaky-box diffusion model, where cosmic-ray escape produces a secondary ratio which falls as:

$$\frac{\phi^-}{\phi^+} \propto \frac{E^{-\delta-\alpha}}{E^{-\alpha}} = E^{-\delta}$$

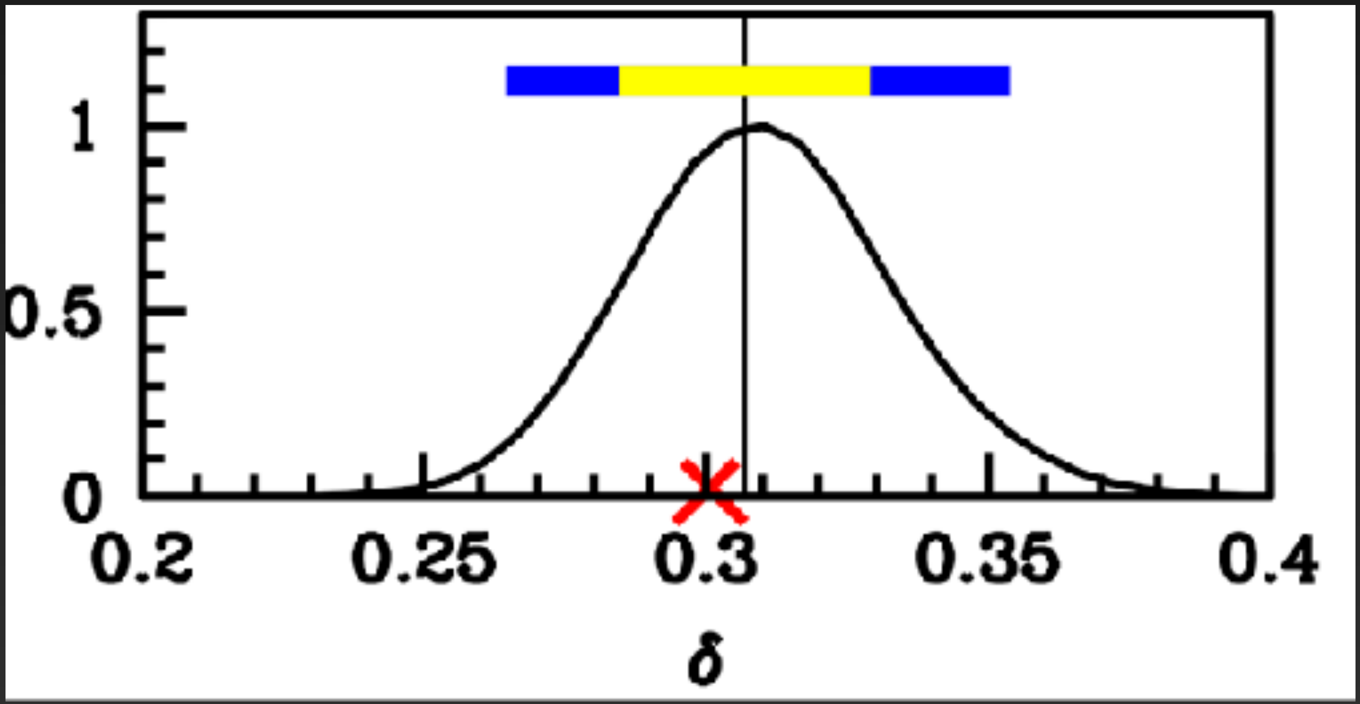

Trotta et al. (2010, 1011.0037)

Stochastic Acceleration

ISM model	K_B^{best}	$K_B^{95\%upper}$	$K_B^{95\%lower}$	χ^2_{tot}	$\chi^2_{d.o.f.}$	$\Delta\chi^2_{tot}$(from back only)
C	6.1	7.6	4.6	34.0	0.68	10.0
E	10.4	12.4	8.1	39.9	0.80	19.7
F	7.4	8.9	5.7	37.5	0.75	20.9

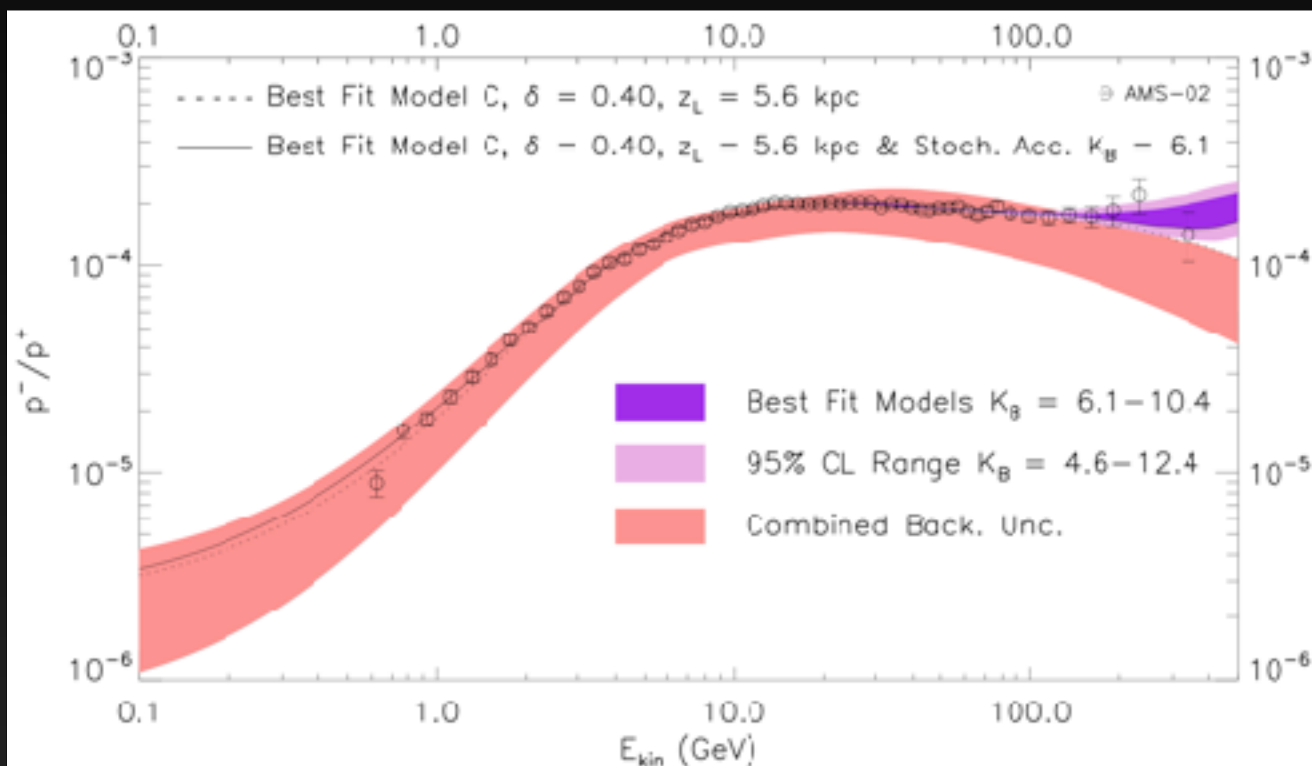

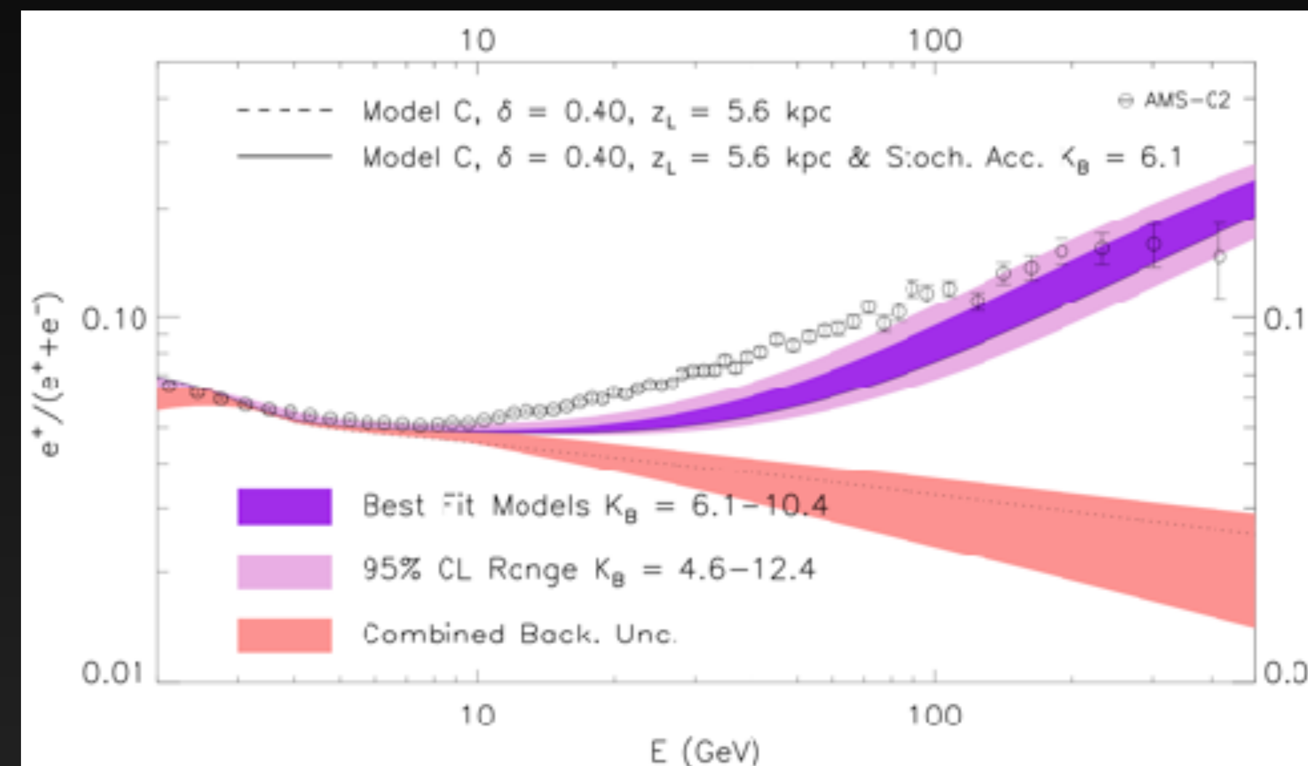

Adding stochastic acceleration hardens the injected antiproton spectrum and improves the fit to the data by 3-4.5σ.

Such a model naturally produces the majority of the rising positron fraction.

HAWC Observations of Pulsars

2HWC Catalog (2017, 1702.02992)

Name	Tested radius [°]	Index	$F_7 \times 10^{15}$ [$\mathrm{TeV^{-1}cm^{-2}s^{-1}}$]	TeVCat
2HWC J0631+169	-	-2.57 ± 0.15	6.7 ± 1.5	Geminga
”	2.0	-2.23 ± 0.08	48.7 ± 6.9	Geminga
2HWC J0635+180	-	-2.56 ± 0.16	6.5 ± 1.5	Geminga
2HWC J0700+143	1.0	-2.17 ± 0.16	13.8 ± 4.2	-
”	2.0	-2.03 ± 0.14	23.0 ± 7.3	-

The intensity of the multi-TeV emission from Geminga and Monogem are surprisingly large.

This indicates that a significant fraction of the total pulsar spin spindown power is transferred into e^+e^- pairs.

Uncertainties in Pair-Conversion Efficiency

On the possibility of efficient production of electron–positron pairs near pulsars and accreting black holes

B. E. Shtern

Institute of Nuclear Research, USSR Academy of Sciences

(Submitted April 16, 1984)

Astron. Zh. **62**, 529–541 (May–June 1985)

The phenomenon of a synchrotron reactor is modeled by the Monte Carlo method under the conditions when the intense production of pairs of electrons and positrons occurs through $\gamma\gamma$ interactions (an electron–positron reactor). The time-dependent solution (particle spectra, electron and positron densities) was calculated under the assumption that the medium is homogeneous under the given initial conditions. It turned out that in a wide range of conditions $\sim 10^{-1}$ of the initial energy injected into the reactor in the form of hard particles goes into the rest mass of electrons and positrons, and the characteristic photon spectrum is established with a sharp dropoff on the high-energy side in the 1 MeV region. Within the framework of the model of an electron–positron reactor the origin of the annihilation γ-ray line, like that observed in the direction of the center of the Galaxy, seems quite natural. Both an accreting black hole (pair production is most efficient if the mass of the hole is $M \lesssim 10^3 M_\odot$) and a young pulsar releasing at least 10^{39} erg/sec in the form of a flux of hard photons from the region of the magnetic poles can serve as the positron source. Other objects for which the development of an electron–positron reactor seems very likely are quasars and active galactic nuclei having a nonthermal luminosity close to the Eddington limit.

And provides an answer to a longstanding mystery

Hooper & Blasi (2009, 0810.1527)

of excess positrons from Geminga alone (3.5×10^{48} erg). We thus conclude that if Geminga were to dominate the observed positron fraction at high energies, it would have to transfer on the order of ~30% of its spin-down power into electron-positron pairs. Such a high efficiency to pairs appears unlikely. The (probably) subdominant role of Geminga is not particularly unexpected, given its relatively old age.

Gelfand et al. (2009, 0904.4053)

SNRs (e.g. Malyshev et al. 2009). If this is correct, the average PWN must deposit $\sim 10^{49}$ ergs of energetic electrons and positrons into the surrounding ISM, and these particles must have an energy spectrum flatter than E^{-2} which extends up to an energy of ~ 1 TeV (Malyshev et al. 2009). For the set of parameters modeled in §3, these conditions are met for only a short period of time during the evolution of this PWN. Using this model, it is possible to determine what sets of neutron star, pulsar wind, supernova, and ISM parameters are required for the PWN to satisfy these criteria for a longer period of time, and evaluate different models for particle escape from the PWN and their effect on the PWN's evolution – particularly if these particles escape gradually or suddenly from the PWN.

Pulsar Energetics

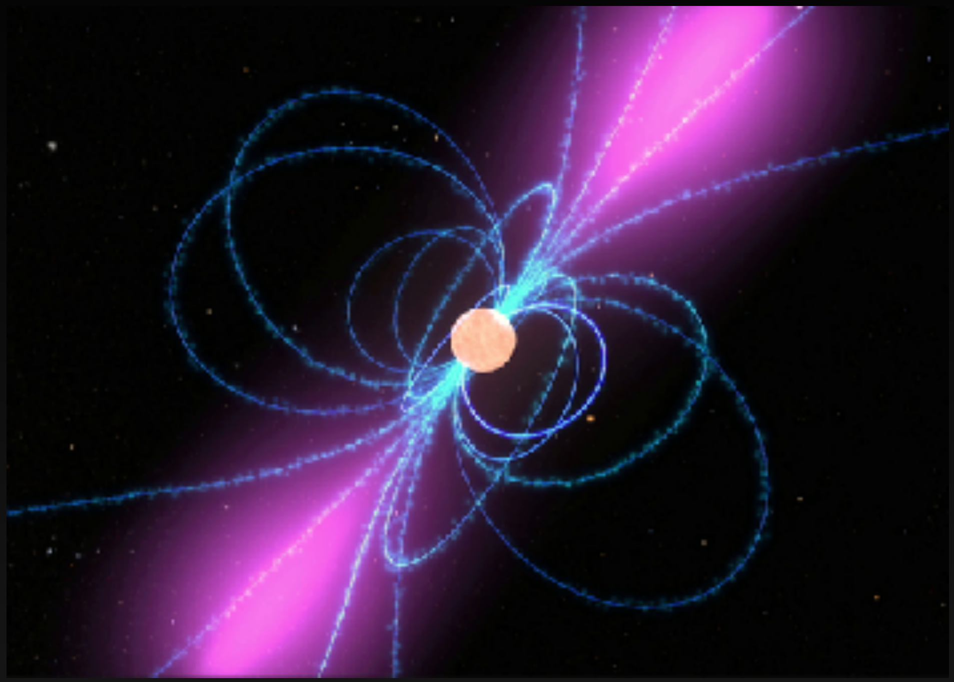

Total Pulsar Spindown Power: ~10^{49} erg
Electron Efficiency: ~10% (HAWC)
Total Electron Injection: ~10^{48} erg

Total Supernova Power: 10^{51} erg
Proton Efficiency: ~10%
Electron to Proton Ratio: ~0.001% - 1% (Cristofari et al. (2013, 1302.2150)
Total Electron Injection: ~10^{45}-10^{48} erg

HAWC Observations of Geminga

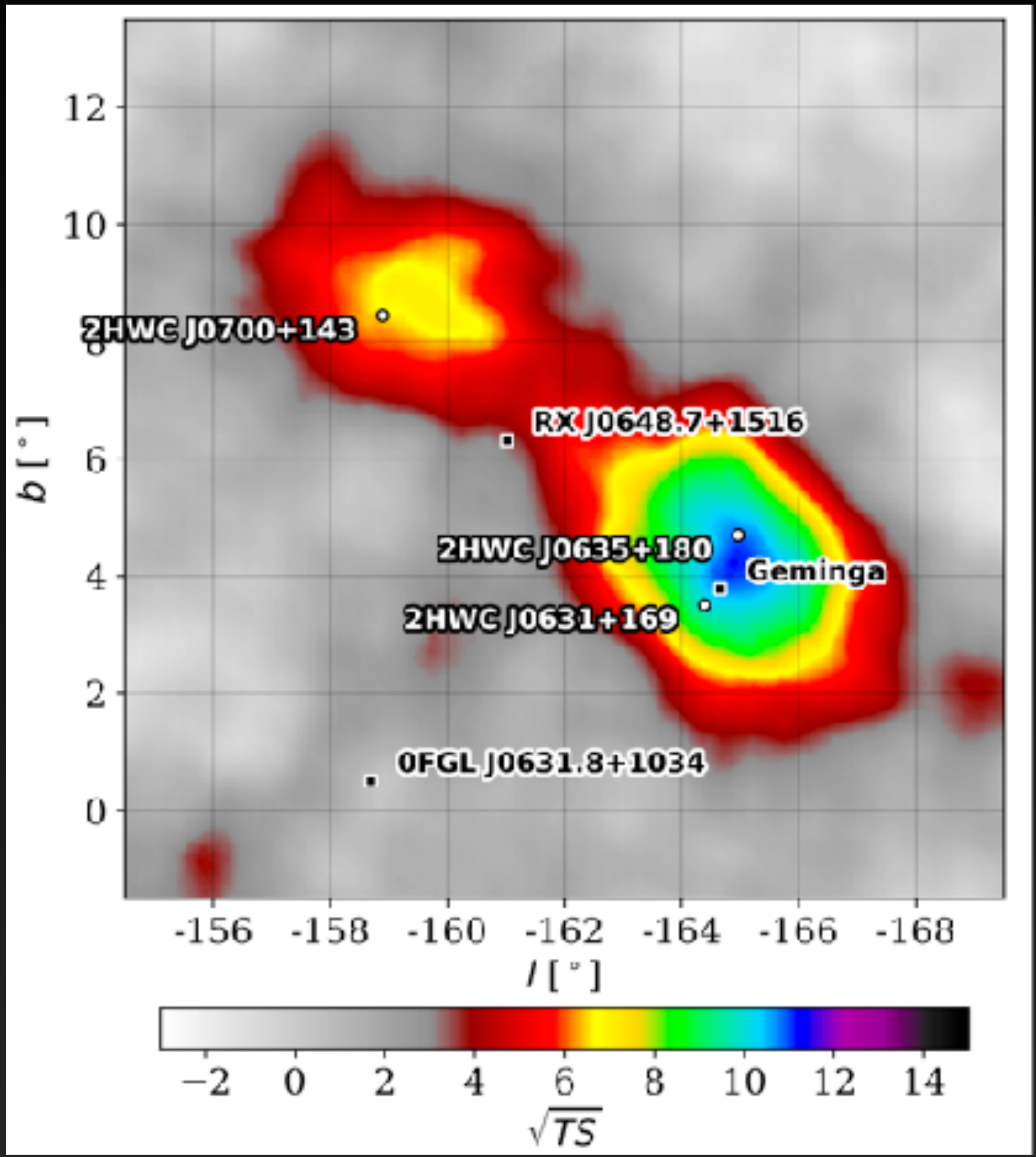

2HWC Catalog (2017, 1702.02992)

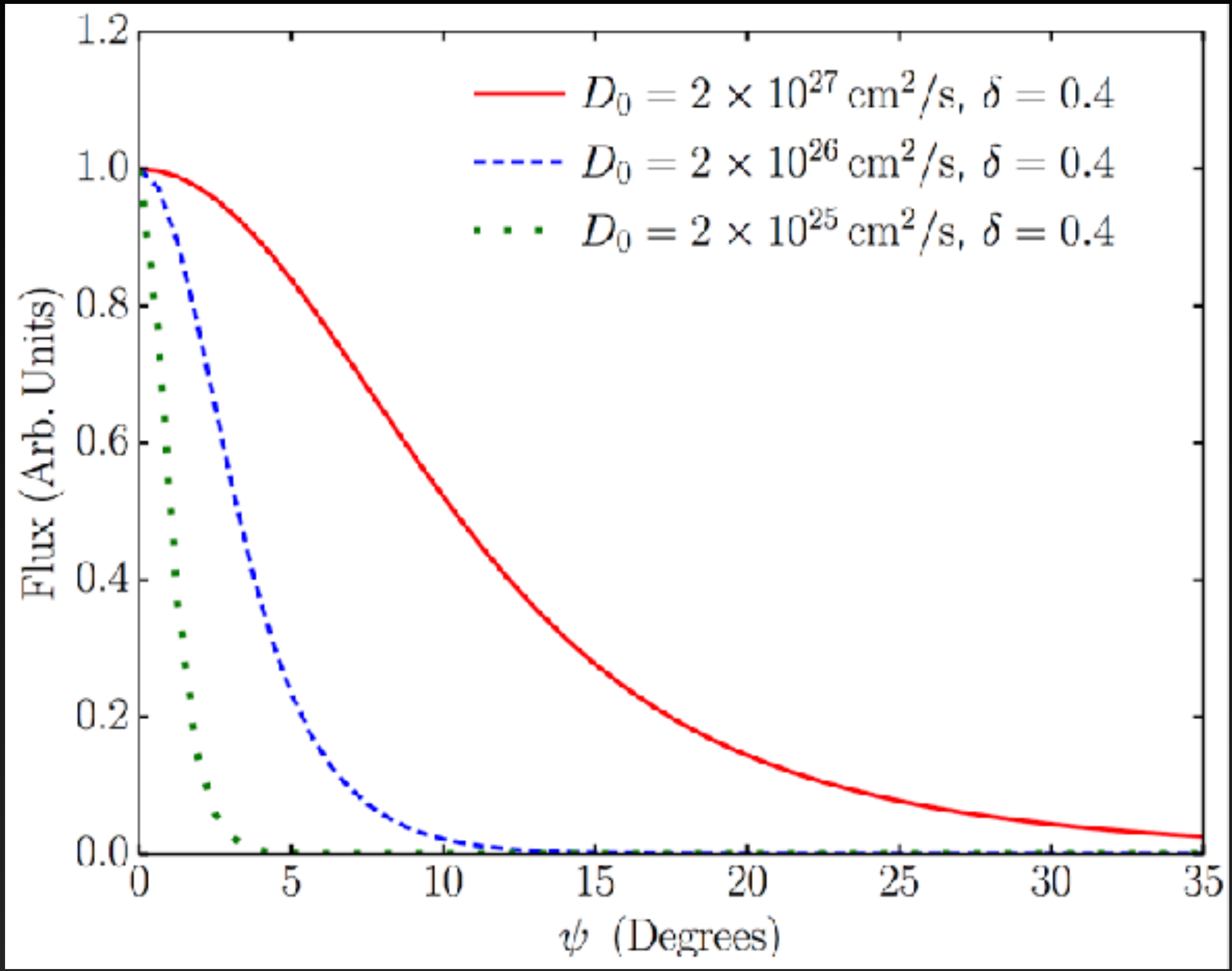

Hooper et al. (2017, 1702.08436)

The large intensity and small spatial extension of this excess indicates that the propagation of leptons is significantly more constrained than in the ISM.

Particle Diffusion From Geminga

Due to the extremely fast energy loss times of high energy electrons, low electrons diffuse farther in most diffusion scenarios.

$$\tau_{Diff} = \frac{L^2}{6D} = \left(\frac{L^2}{6D_0}\right) E^{-\delta}$$

$$\tau_{loss} \propto (\phi_B + \phi_{ISRF})\, E^{-1}$$

$$\frac{\Delta E}{E} \approx \frac{\tau_{Diff}}{\tau_{loss}} \propto E^{1-\delta}$$

δ = 1.0 (Bohmian diffusion)

δ = 0.5 (Kraichnan diffusion)

δ = 0.33 (Kolmogorov diffusion)

δ = 0.0 (Convection*)

* at a single distance

Energy Losses Near Geminga

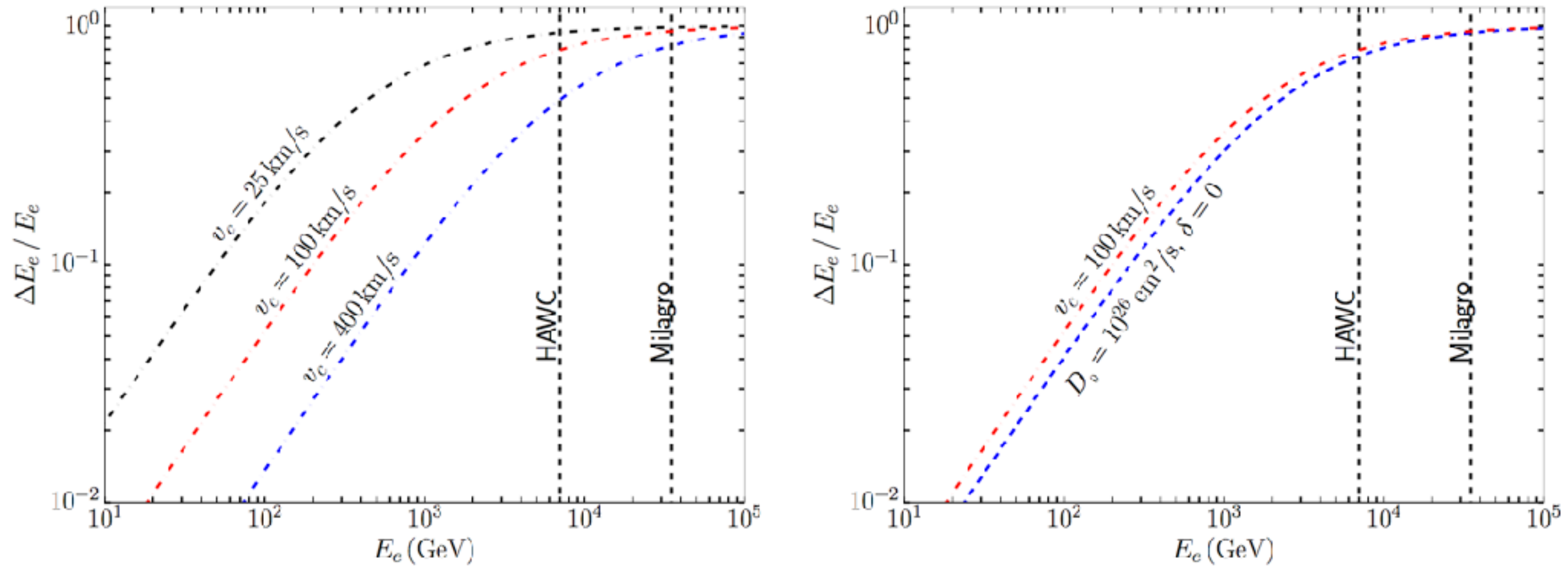

The intensity of the multi-TeV emission from Geminga and Monogem are surprisingly large.

This indicates that a significant fraction of the total pulsar spin spindown power is transferred into e^+e^- pairs.

Fitting the Geminga TeV Spectrum

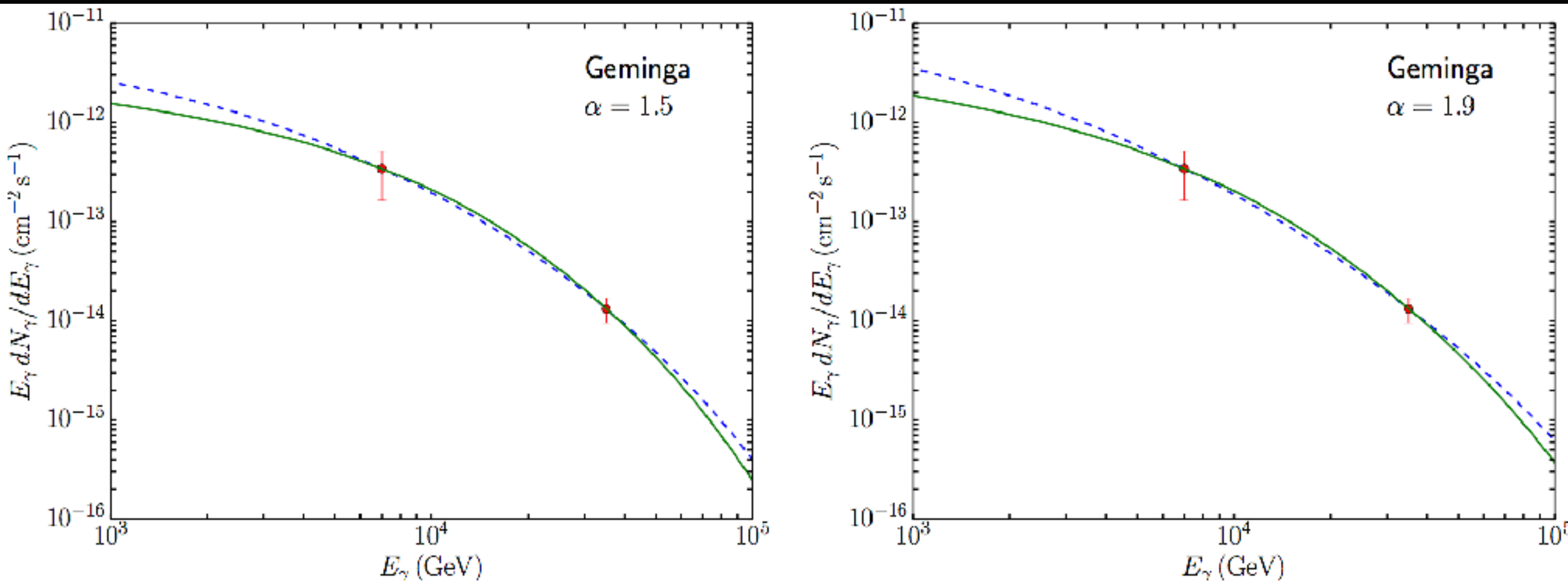

Low (blue dotted) and high (green solid) convection:

Spectral Slope (low-convection): -2.47 (α=1.5), -2.59 (α=1.9)

Spectral Slope (high-convection): -2.23 (α=1.5), -2.32 (α=1.9)

HAWC Data: -2.23 +/- 0.08

The Diffusion Region Around Geminga

Due to the extremely fast energy loss times of high energy electrons, low electrons diffuse farther in most diffusion scenarios.

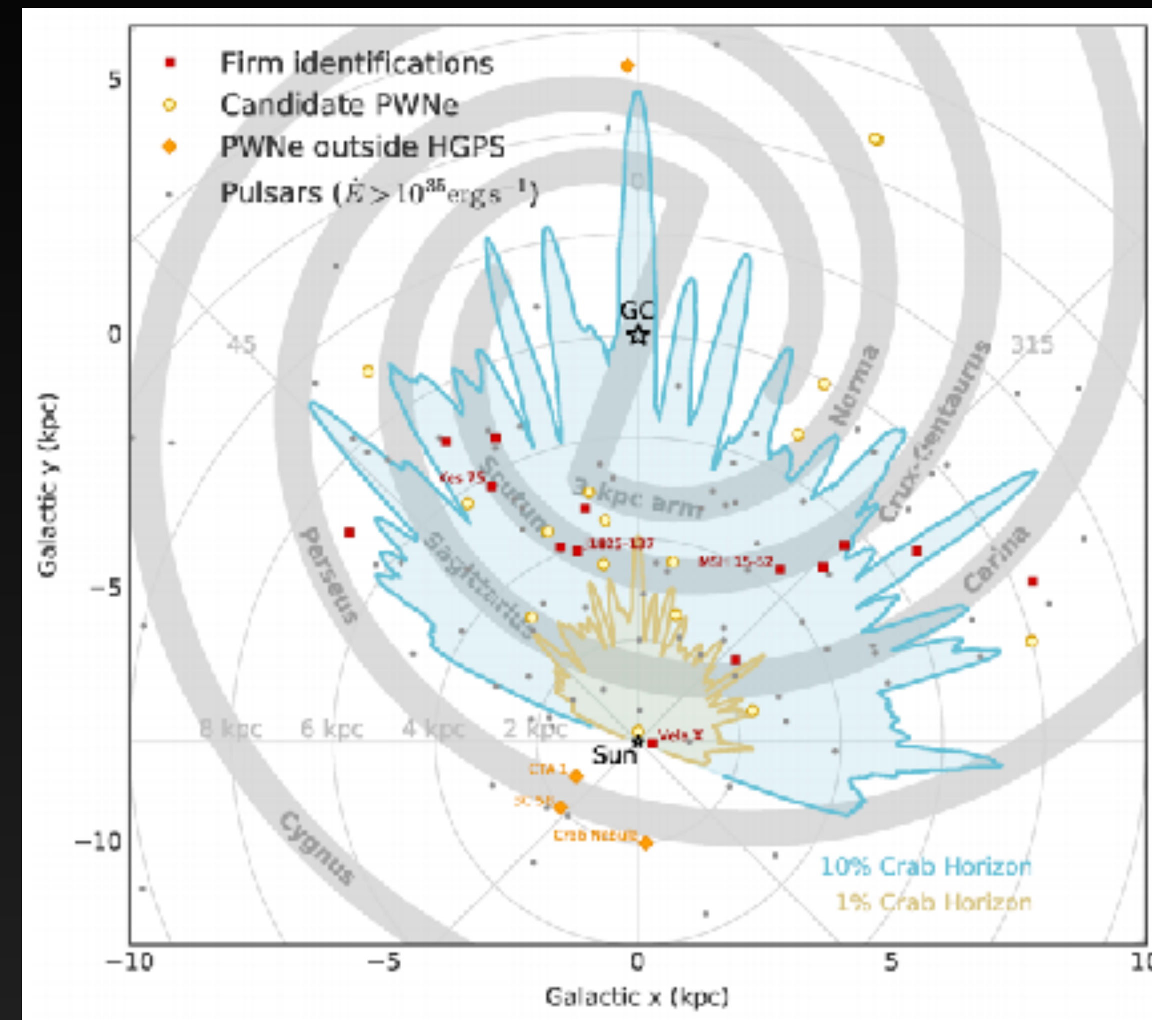

$$f \sim \frac{N_{\rm region} \times \frac{4\pi}{3} r_{\rm region}^3}{\pi R_{\rm MW}^2 \times 2 z_{\rm MW}}$$

$$\sim 0.25 \times \left(\frac{r_{\rm region}}{100\,{\rm pc}}\right)^3 \left(\frac{\dot{N}_{\rm SN}}{0.03\,{\rm yr}^{-1}}\right) \left(\frac{\tau_{\rm region}}{10^6\,{\rm yr}}\right) \left(\frac{20\,{\rm kpc}}{R_{\rm MW}}\right)^2 \left(\frac{200\,{\rm pc}}{z_{\rm MW}}\right)$$

Quantity	Best fit value	Posterior mean and standard deviation	Posterior 95% range
DIFFUSION MODEL PARAMETERS Θ			
$D_0 (10^{28}\ {\rm cm}^2\ {\rm s}^{-1})$	6.59	8.32 ± 1.46	$[5.45, 11.20]$
δ	0.30	0.31 ± 0.02	$[0.26, 0.35]$
$v_{\rm Alf}$ (km s^{-1})	39.2	38.4 ± 2.1	$[34.2, 42.7]$
z_h (kpc)	3.9	5.4 ± 1.4	$[3.2, 8.6]$
ν_1	1.91	1.92 ± 0.04	$[1.84, 2.00]$
ν_2	2.40	2.38 ± 0.04	$[2.29, 2.47]$
N_p (10^{-9} cm^2 sr^{-1} s^{-1} MeV^{-1})	5.00	5.20 ± 0.48	$[4.32, 6.23]$

Trotta et al. (2011, 1011.0037)

Is Geminga Unique?

$$\tau_{Diff} = \frac{L^2}{6D} = \left(\frac{L^2}{6D_0}\right) E^{-\delta}$$

$$\tau_{loss} \propto (\phi_B + \phi_{ISRF})\, E^{-1}$$

If $D_0 = 1.0 \times 10^{26}$ cm^{2}s^{-1} in a region around Earth, the diffusion of 1 TeV electrons is:

$$\tau_{Diff} = 500 \text{ kyr} \left(\frac{r}{100pc}\right)^2$$

$$\tau_{loss} = 300 \text{ kyr}$$

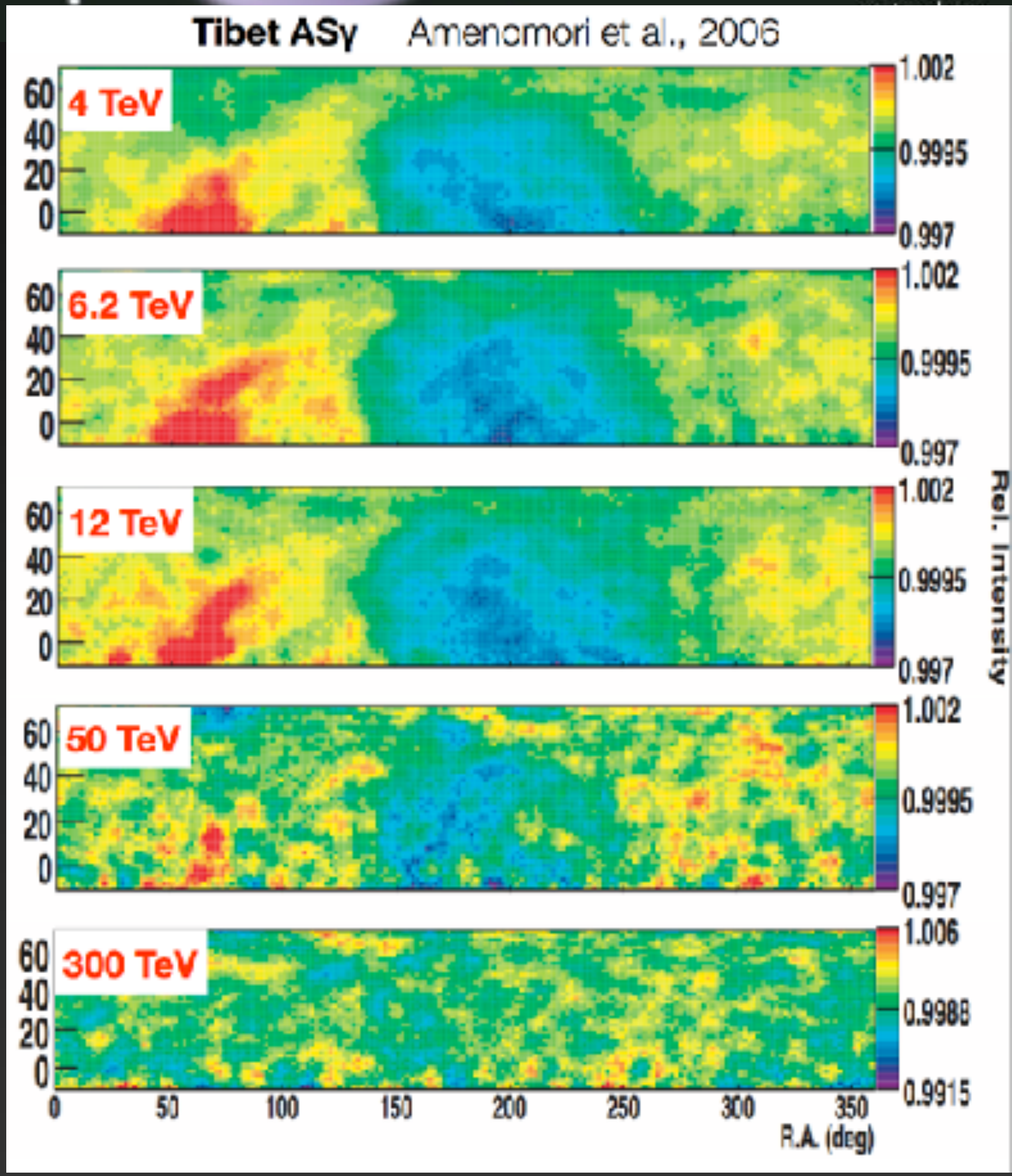

HAWC Observations of Geminga

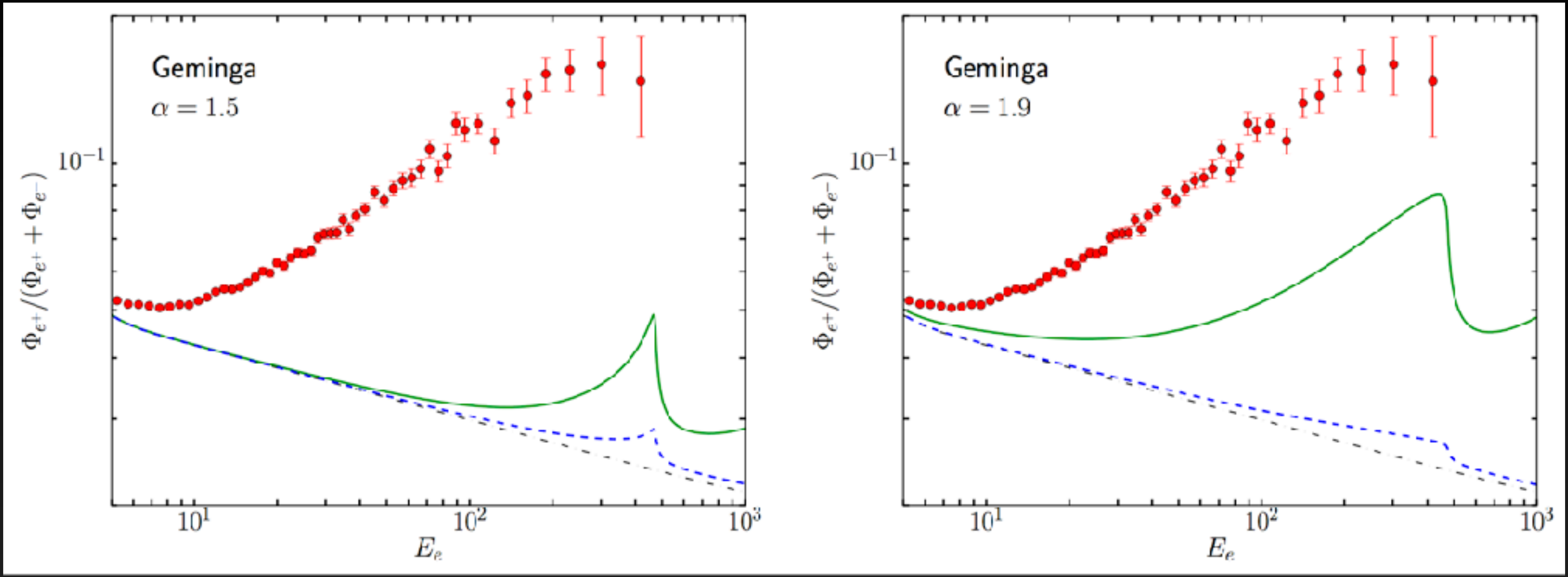

Assuming standard galactic diffusion, Geminga provides a reasonable contribution to the positron excess.

Note: The majority of these electrons were emitted in the first ~100 kyr of Geminga evolution, the electrons emitted today don't contribute!

HAWC Observations of Geminga

It is not surprising that Geminga produces only a small portion the excess - other pulsars contribute too!

Monogem produces the highest energy e^+e^-, because it is younger.

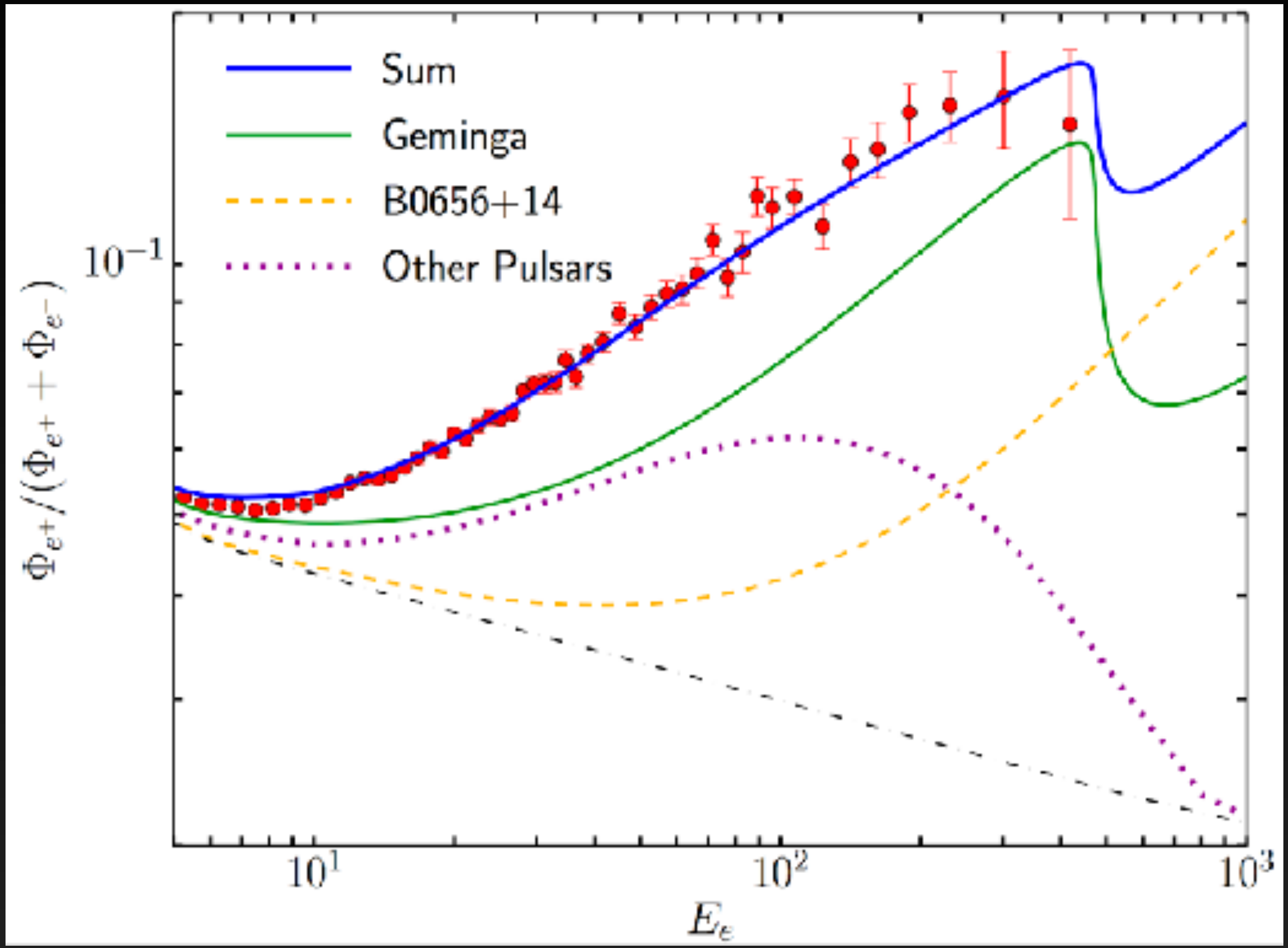

The average pulsar in the field provides the majority of low-energy positrons.

Recent Fermi-LAT Measurements

Fermi-LAT Collaboration (2017)

Recent (yesterday) Fermi-LAT measurements continue the hardening of the e^{+}+e^{-} flux up to 2 TeV.

Constraints on the anisotropy are beginning to enter an interesting parameter space.

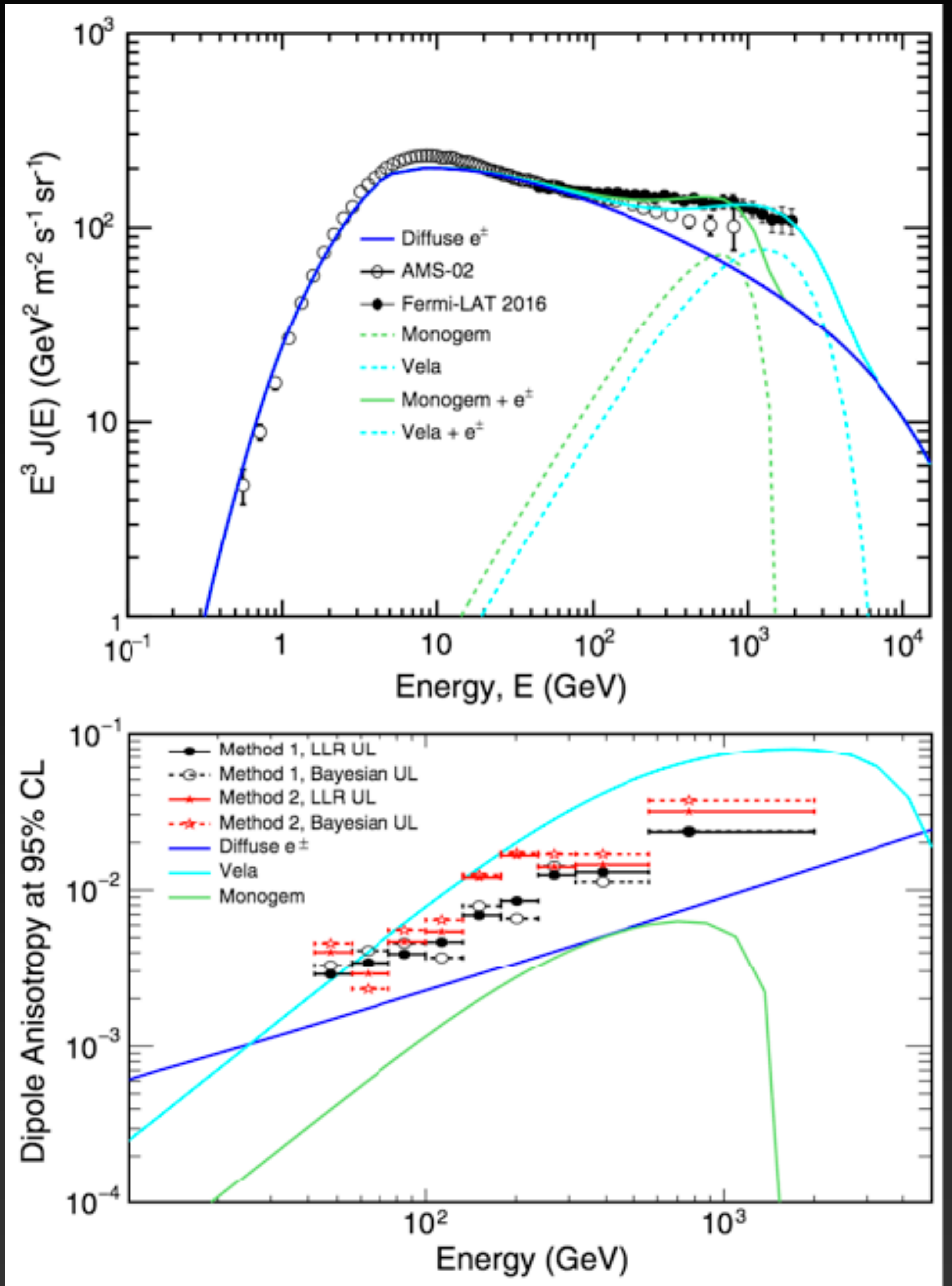

Future Work (Anisotropy)

One method to disentangle these contributions is to search for anisotropies in the cosmic-ray lepton intensity

$$\Delta = \frac{3}{2c}\frac{d}{T}\frac{(1-\delta)E/E_{\rm loss}}{1-(1-E/E_{\rm loss})^{1-\delta}}\frac{N_{\rm psr}(E)}{N_{\rm tot}(E)}$$

These searches are sensitive because misidentified hadronic backgrounds are a statistical, not systematic, error:

$$N_{tot} = (N_{psr} + N_{\gamma}) + (N_{e,iso} + N_p)$$

$$\Delta = \frac{N_f - N_b}{N_f + N_b} = \frac{N_{psr,f} - N_{psr,b}}{N_{psr,f} + N_{psr,b} + 2(N_{e,iso} + N_p)}$$

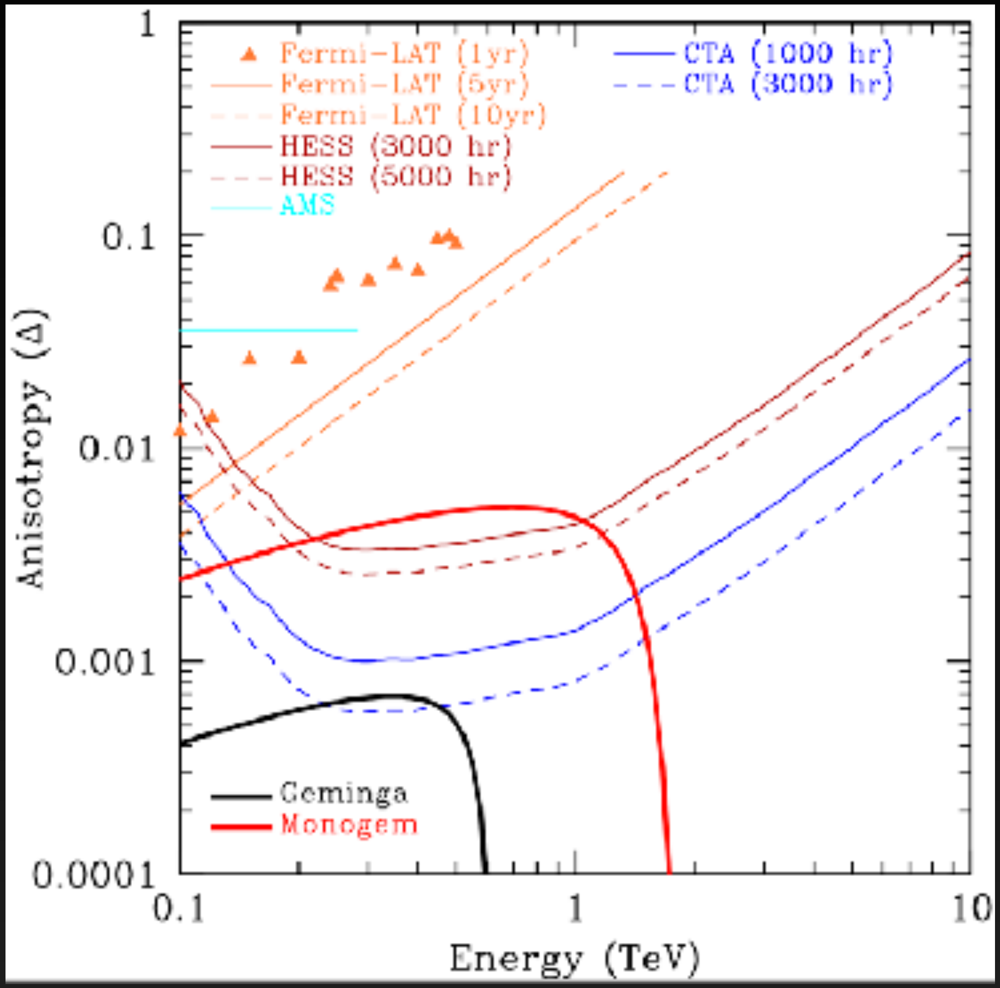

Linden & Profumo (2013, 1304.1791)

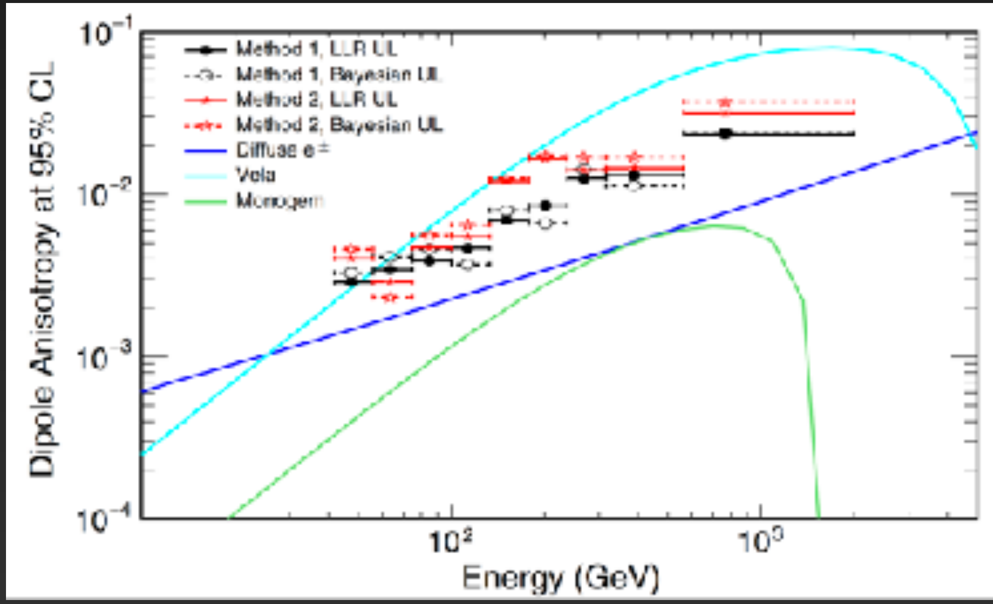

Fermi-LAT Collaboration (2017)

Future Work (TeV PWN)

For the Rest of this Talk I Will Assume:

1.) A significant fraction of the pulsar spin-down power is converted into e+e- pairs, and this powers the extended TeV emission observed by Geminga and Monogem.

2.) This emission is a generic feature of 100-300 kyr pulsars.

These emission halos thus act as the TeV analogs of PWN

Auchettl et al. (2017, To Be Submitted)

Future Work (TeV PWN)

I will argue that HAWC is likely to already be seeing TeV pulsar nebulae that have not yet been observed at other wavelengths.

These sources are likely to be among the closest pulsars, and are thus important for the positron excess.

Auchettl et al. (2017, To Be Submitted)

Pulsar Detections

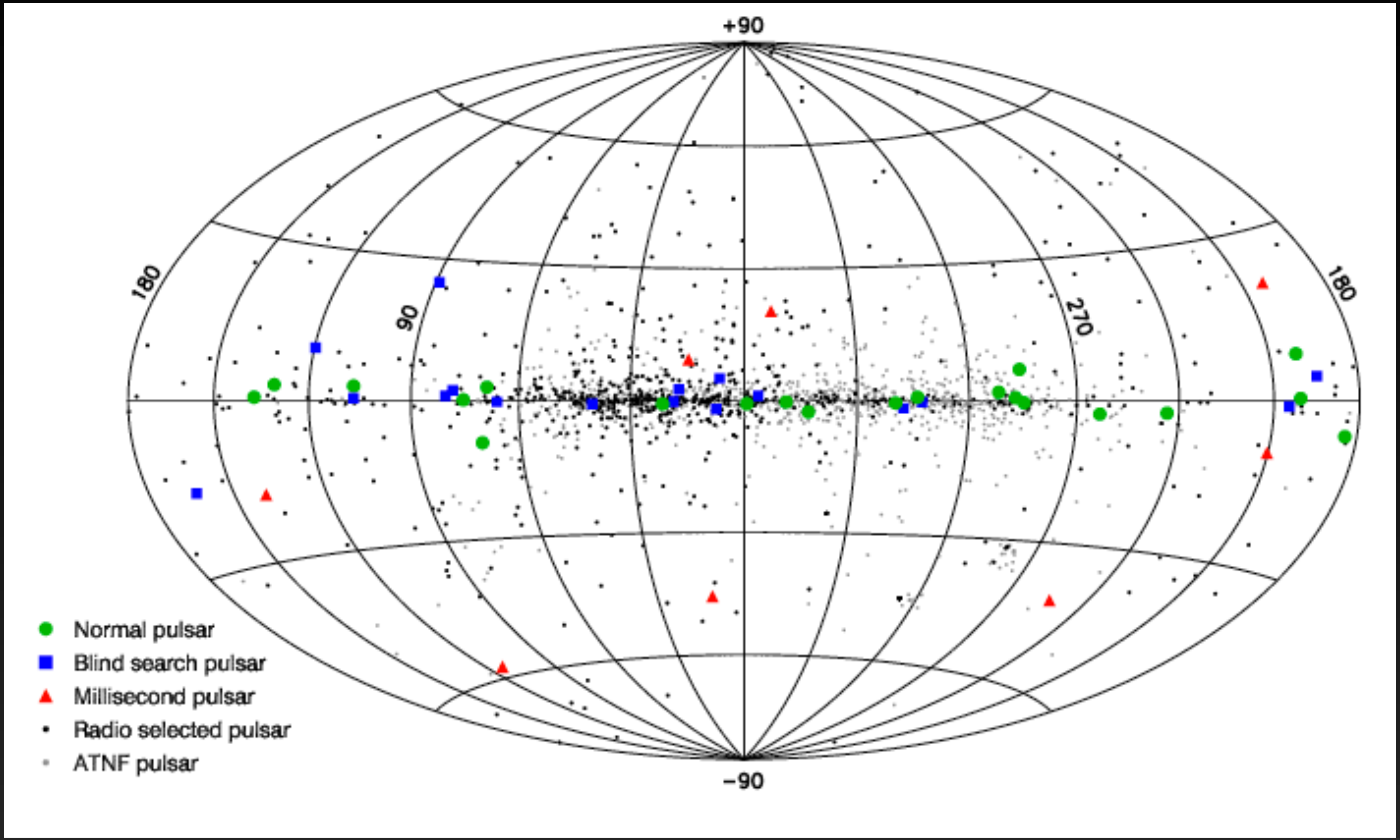

Radio observations have been extremely efficient at finding galactic pulsars, the ATNF catalog contains >2500 sources

Is this everything?

Pulsar Detections

Tauris and Manchester (1998) find that the beam window for young pulsars is approximately:

$$\theta = 8^\circ \sqrt{\frac{1\ \mathrm{s}}{P}}$$

This implies that ~90% of pulsars are not detected in radio

Missing Pulsars

Models of the pulsar distribution of by Lorimer et al. anticipate a population exceeding 20 pulsars within 1 kpc of the sun

Instead, only 9 ATNF pulsars are detected with t < 300 kyr and d < 1 kpc.

Additionally Fermi-LAT measurements of radio quiet pulsars indicate that we are missing many systems.

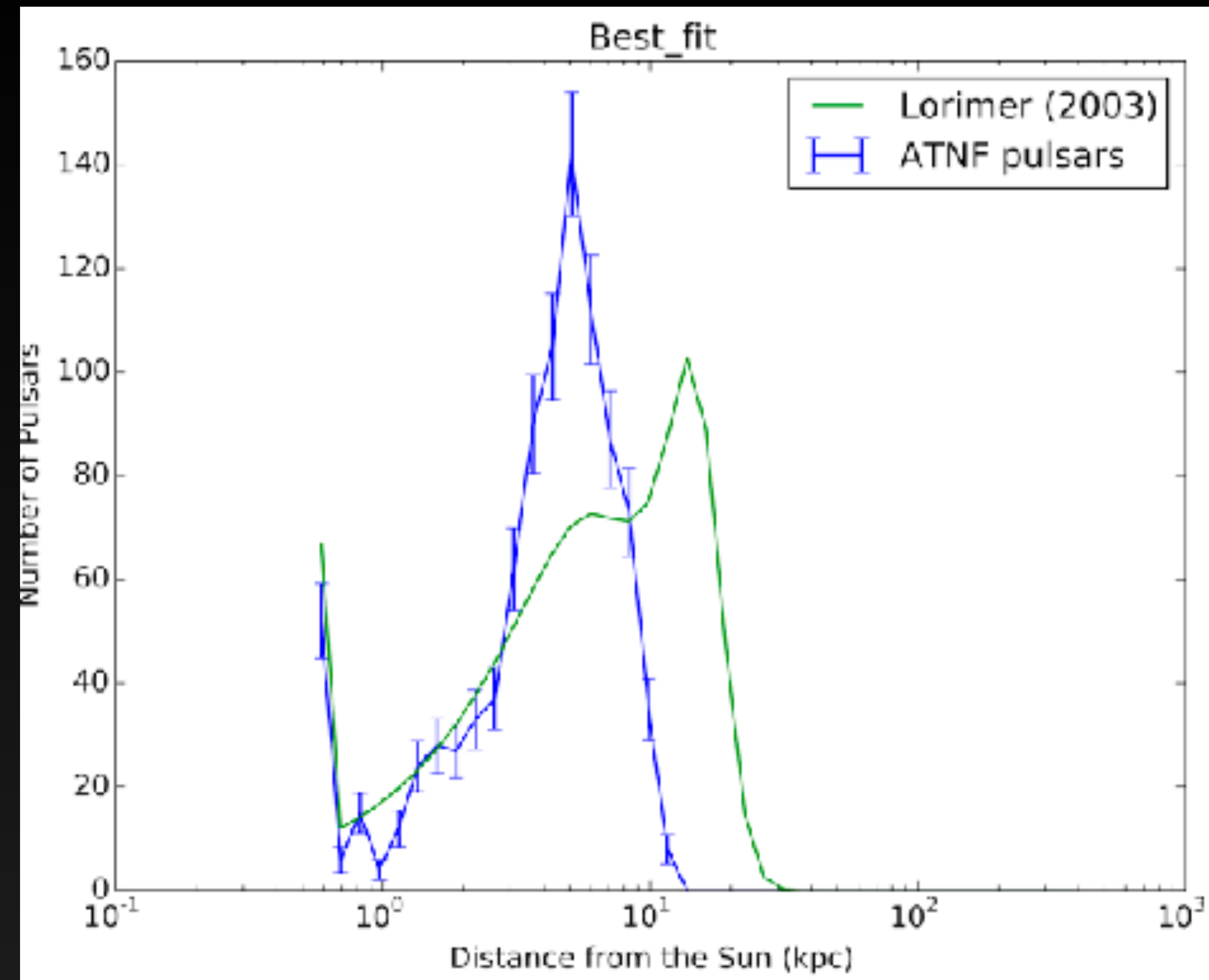

#	NAME		DIST (kpc)	AGE (Yr)
1	B0656+14	mlt+78	0.29	1.11e+05
2	B0833-45	lvm68	0.28	1.13e+04
3	J0940-5428	mlc+01	0.38	4.22e+04
4	J0954-5430	mlc+01	0.43	1.71e+05
5	B1001-47	mlt+78	0.37	2.2e+05
6	J1732-3131	aaa+09c	0.64	1.11e+05
7	B1737-30	cl86	0.40	2.06e+04
8	B1822-09	dls72	0.30	2.32e+05
9	B2334+61	dtws85	0.70	4.06e+04

Pulsar Wind Nebulae

PWN should also produce isotropic emission, and can be detected with sensitive X-Ray telescopes.

However, few PWN without associated pulsars have been detected.

The majority of PWN are within 1° of the Galactic plane, which should bias us against the closest pulsars.

Table 7.6. *PWNe With No Detected Pulsar*

Nebula	other name	d (kpc)	M	S	γ	Reference
G0.13−0.11		?	M	N	?	Wang et al. 02
G0.9+0.1		8	T	Y	N	Porquet 03
G7.4−2.0	GeV J1809−2327	1.9	J	?	Y	Braje et al. 02
G16.7+0.1		2.2	M	Y	N	Helfand et al. 03
G18.5−0.4	GeV J1825−1310	4.1	J	?	Y	Roberts et al. 01
G20.0−0.2		5.4	?	N	N	Becker & Helfand 85a
G21.5−0.9		5.5	M	N	N	Slane et al. 00
G24.7+0.6			?	N	N	Reich et al. 84
G27.8+0.6			?	N	N	Reich et al. 84
G39.2−0.3	3C 396	7.7	M	Y	Y	Olbert et al. 03
G63.7+1.1		3.8	?	N	N	Wallace et al. 97
G74.9+1.2	CTB 87	12	M	N	Y	Mukherjee et al. 00
G119.5+10.2	CTA 1	2.1	M	Y	Y	Slane et al. 03
G189.1+3.0	IC 443	1.5	J	Y	?	Olbert et al. 01
G279.8−35.8	B0453−685	50	M	Y	N	Gaensler et al. 03
G291.0−0.1	MSH 11−62	?	J	Y	Y	Harrus et al. 03
G293.8+0.6			?	Y	N	Whiteoak & Green 96
G313.3+0.1	Rabbit	?	J	N	Y	Roberts et al. 99
G318.9+0.4			?	Y	N	Whiteoak & Green 96
G322.5−0.1			?	Y	N	Whiteoak & Green 96
G326.3−1.8	MSH 15−56	4.1	?	Y	N	Dickel et al. 00
G327.1−1.1		8.8	M	Y	N	Bocchino & Bandiera 03
G328.4+0.2	MSH 15−57	> 17	M	N	N	Hughes et al. 00
G359.89−0.08		8	J	N	Y	Lu et al. 03

Kaspi et al. (2004, astro-ph/0402136)

HESS Observations of PWN

Table 4 Candidate pulsar wind nebulae from the pre-selection.

HGPS name	ATNF name	lg $\dot{E}$	τ_c (kyr)	d (kpc)	PSR offset (pc)	Γ	R_{PWN} (pc)	$L_{1-10\ \mathrm{TeV}}$ (10^{33} erg s^{-1})	Rating 1	2	3	4
J1616−508 (1)	J1617−5055	37.20	8.13	6.82	< 26	2.34 ± 0.06	28 ± 4	162 ± 9	★	★	★	★
J1023−575	J1023−5746	37.04	4.60	8.00	< 9	2.36 ± 0.05	23.2 ± 1.2	67 ± 5	★	★	★	★
J1809−193 (1)	J1811−1925	36.81	23.3	5.00	29 ± 7	2.38 ± 0.07	35 ± 4	53 ± 3	★	★	★	↯
J1857+026	J1856+0245	36.66	20.6	9.01	21 ± 6	2.57 ± 0.06	41 ± 9	118 ± 13	★	★	★	★
J1640−465	J1640−4631 (1)	36.64	3.35	12.8	< 20	2.55 ± 0.04	25 ± 8	210 ± 12	★	★	★	★
J1641−462	J1640−4631 (2)	36.64	3.35	12.8	50 ± 5	2.50 ± 0.11	< 14	17 ± 4	↯	⋆	★	⋆
J1708−443	B1706−44	36.53	17.5	2.60	17 ± 3	2.17 ± 0.08	12.7 ± 1.4	6.6 ± 0.9	★	★	★	★
J1908+063	J1907+0602	36.45	19.5	3.21	21 ± 3	2.26 ± 0.06	27.2 ± 1.5	28 ± 2	★	★	★	★
J1018−589A	J1016−5857 (1)	36.41	21.0	8.00	47.5 ± 1.6	2.24 ± 0.13	< 4	8.1 ± 1.4	↯	⋆	★	⋆
J1018−589B	J1016−5857 (2)	36.41	21.0	8.00	25 ± 7	2.20 ± 0.09	21 ± 4	23 ± 5	★	★	★	★
J1804−216	B1800−21	36.34	15.8	4.40	18 ± 5	2.69 ± 0.04	19 ± 3	42.5 ± 2.0	★	★	★	★
J1809−193 (2)	J1809−1917	36.26	51.3	3.55	< 17	2.38 ± 0.07	25 ± 3	26.9 ± 1.5	★	★	★	★
J1616−508 (2)	B1610−50	36.20	7.42	7.94	60 ± 7	2.34 ± 0.06	32 ± 5	220 ± 12	↯	★	★	★
J1718−385	J1718−3825	36.11	89.5	3.60	5.4 ± 1.6	1.77 ± 0.06	7.2 ± 0.9	4.6 ± 0.8	★	★	★	★
J1026−582	J1028−5819	35.92	90.0	2.33	9 ± 2	1.81 ± 0.10	5.3 ± 1.6	1.7 ± 0.5	↯	★	★	★
J1832−085	B1830−08 (1)	35.76	147	4.50	23.3 ± 1.5	2.38 ± 0.14	< 4	1.7 ± 0.4	↯	↯	★	⋆
J1834−087	B1830−08 (2)	35.76	147	4.50	32.3 ± 1.9	2.61 ± 0.07	17 ± 3	25.8 ± 2.0	↯	★	★	↯
J1858+020	J1857+0143	35.65	71.0	5.75	38 ± 3	2.39 ± 0.12	7.9 ± 1.6	7.1 ± 1.5	↯	★	★	↯
J1745−303	B1742−30 (1)	33.93	546	0.200	1.42 ± 0.15	2.57 ± 0.06	0.62 ± 0.07	0.014 ± 0.003	↯	↯	★	↯
J1746−308	B1742−30 (2)	33.93	546	0.200	< 1.1	3.3 ± 0.2	0.56 ± 0.12	0.009 ± 0.003	⋆	↯	★	↯

HESS Collaboration (2017, 1702.08280)

Further motivating this model, we note that HESS has seen numerous TeV PWN

HAWC Sensitivity to Geminga/Monogem

The extended Geminga and Monogem sources lie far above the HAWC sensitivity threshold:

The extended Geminga and Monogem sources lie far above the HAWC sensitivity threshold (though they are extended)

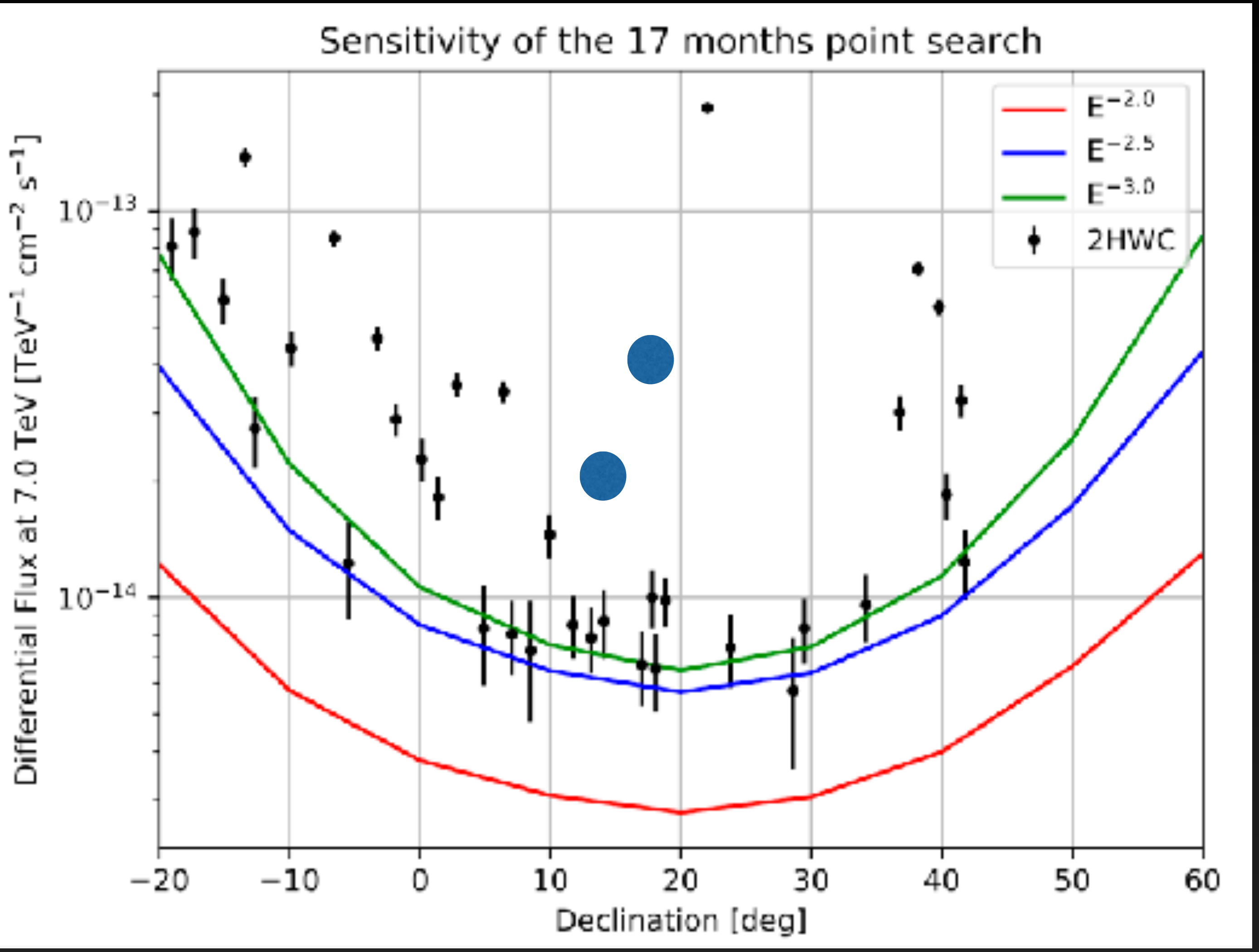

HAWC Collaboration (2017, 1702.02992)

We could see these sources to much greater distances – if they are farther away they will be more point like, improving the sensitivity:

$d_{Geminga}$ ~ 950 pc (650 pc) @ 20° (50°)

$d_{Monogem}$ ~ 650 pc (450 pc) @ 20° (50°)

Following Up HAWC Sources

ROSAT searches already produce some intriguing hints:

Extended ~ 1°
HESS J1813-178 (PWN)?

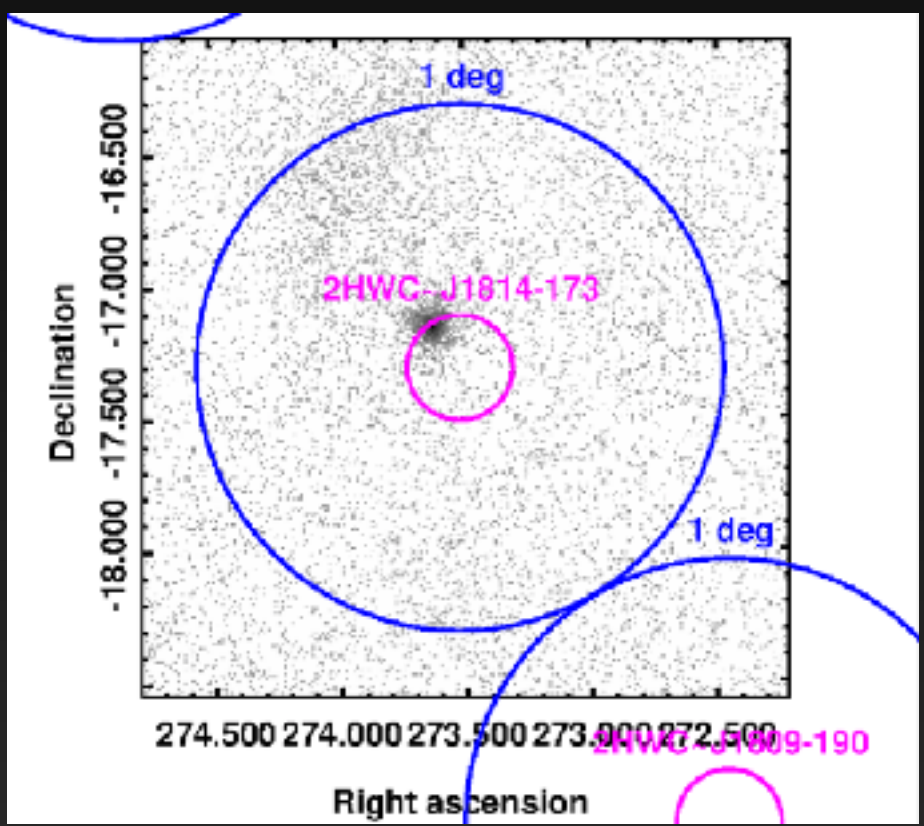

Extended ~ 0.8°
HESS J1849-000 (PWN)?
IGR J18490-0000

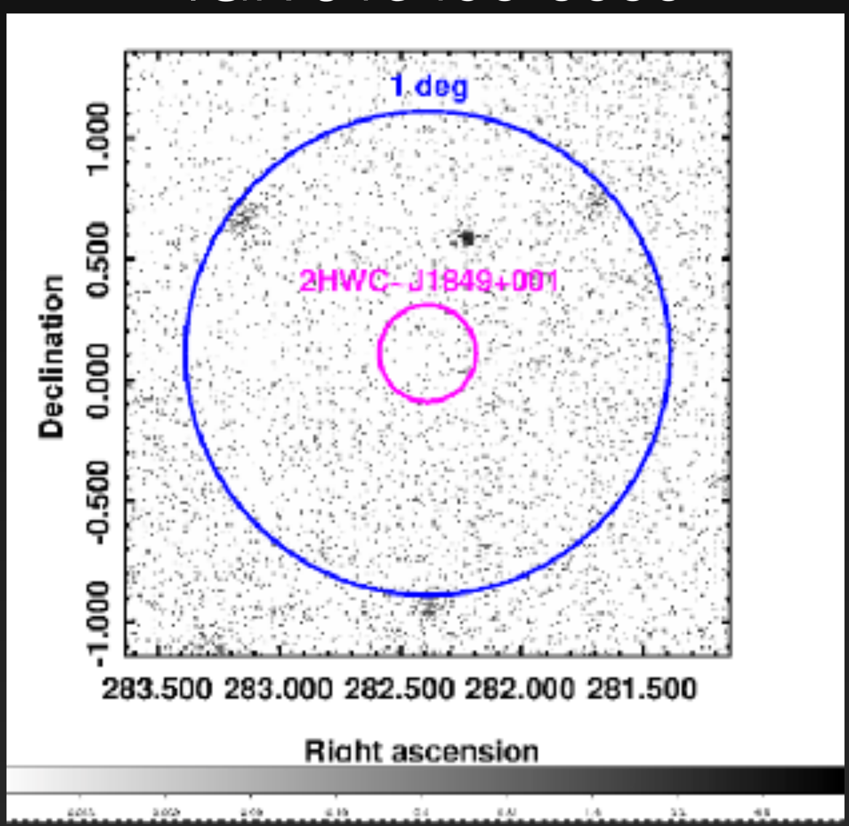

Extended ~ 0.7°
TeV J2032+4130(PWN)?

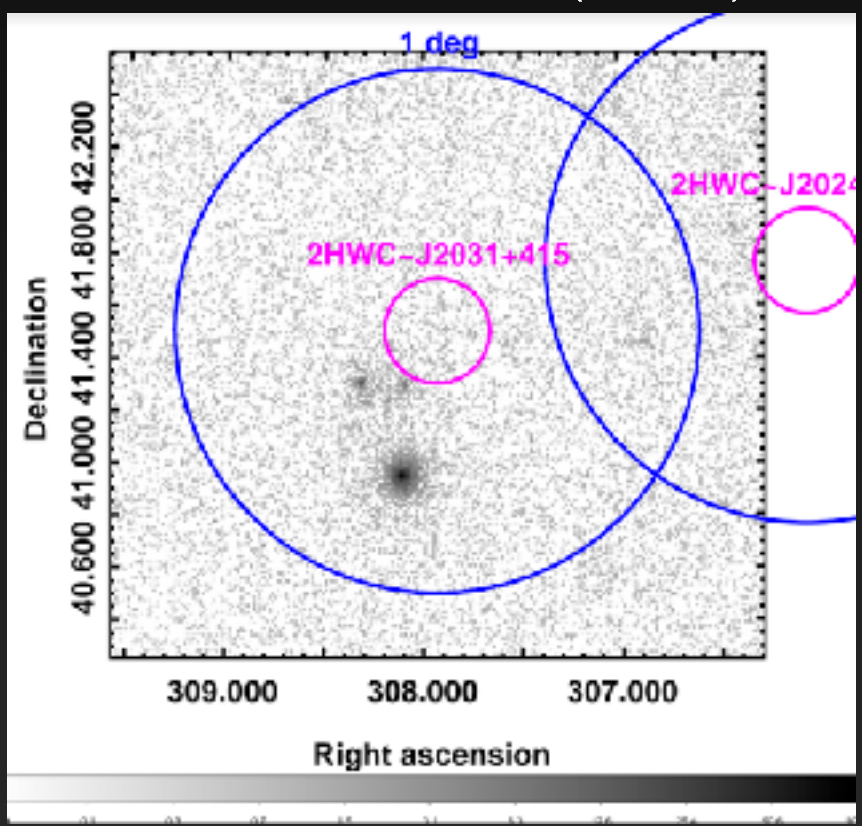

Deeper, high-resolution X-Ray searches could begin to see similar associations in currently unknown HAWC sources.

Optical Searches

Prinz & Becker (2016, 1511.07713)

In addition to X-Ray detections of the PWN, optical detections of the pulsar point-source are possible:

$$10^5 - 10^6 \text{ K} = 8 - 80 \text{ eV}$$

Observations from Hubble can detect these systems within several hundred pc.

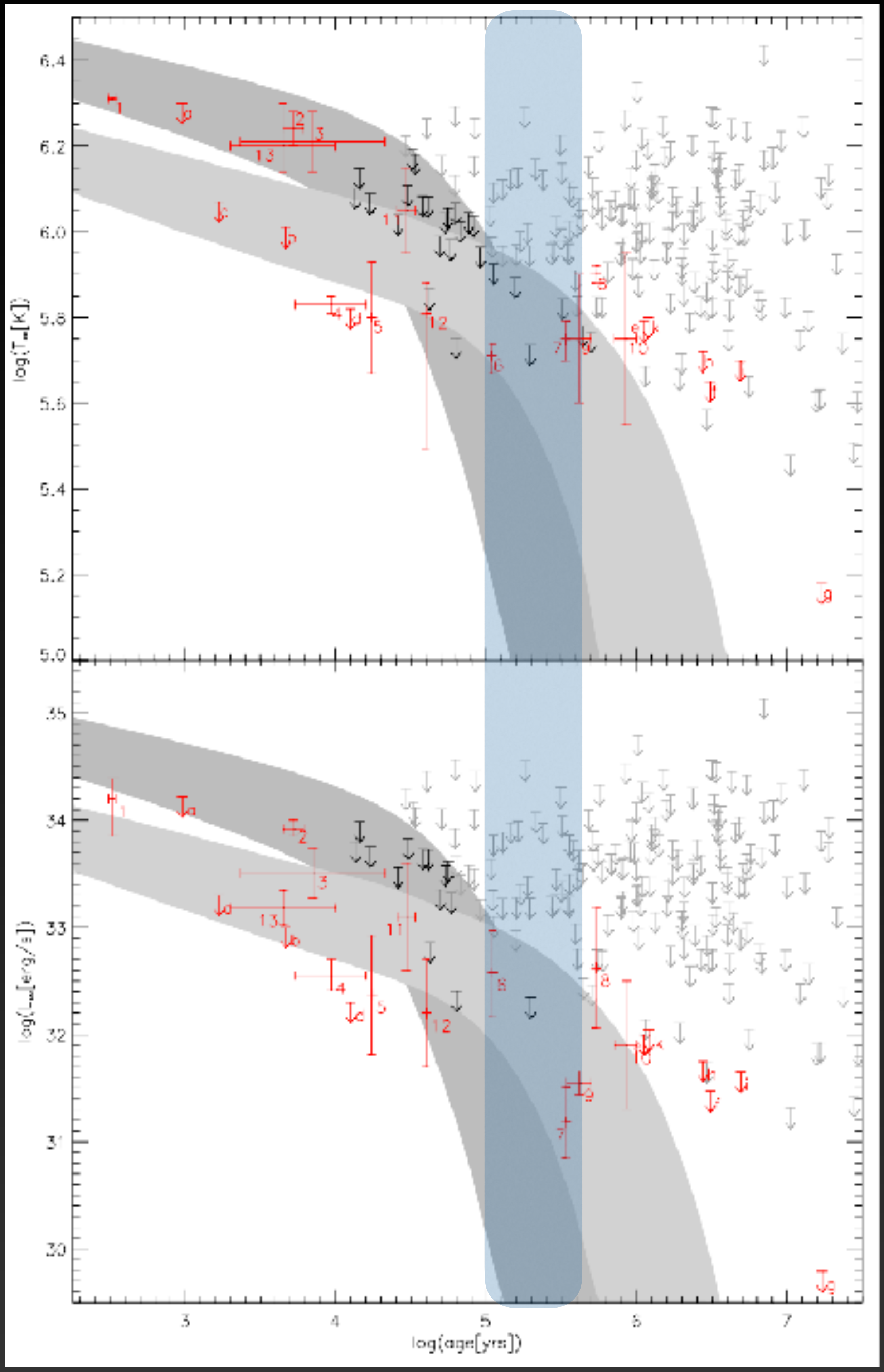

The Future

These observations can answer a number of questions:

1.) Is an X-Ray PWN necessary to produce a TeV nebula?

2.) What is the beaming fraction of mature pulsars in radio/X-Ray/gamma-ray energies?

3.) What is the breaking index and spin-down power of pulsars?

4.) What is the contribution of pulsars to the positron excess?


TeVPA 2017
August 7 - 11
SHORT NORTH
THE OHIO STATE UNIVERSITY
CENTER FOR COSMOLOGY AND
ASTROPARTICLE PHYSICS

Propose a Mini-Workshop!

</> Conference Invitation | Pre-Conference Mini-Workshops | Code of Conduct

Pre-Conference Mini-Workshops

We want to make TeVPA an opportunity for the community to get together to tackle open problems that require the combined input from different experimental collaborations and theorists.

To help achieve this, we are planning to host a number of informal pre-conference mini-workshop sessions, either on Saturday, August 5th or Sunday, August 6th. Each session would address a particular open problem. Potential topics are, for instance, "the anisotropic sky", "the Galactic Center excess", "high-energy astrophysical neutrino sources", and "UHECR sources"; the list is non-exhaustive. There would maybe be one or two short presentations. Most of the time should be dedicated to discussion and to collaboration within and between different experiments.

Attendees would be a subset of the TeVPA participants that are working on these problems or interested in them. Each session would be made up of members of cosmic-ray, gamma-ray, gravitational-wave, and neutrino collaborations, plus independent theorists. CCAPP would provide meeting rooms, facilities, and coffee breaks.

If you are interested in proposing, attending, or planning a mini-workshop broadly centered on TeV Particle Astrophysics, please contact us at tevpa2017@osu.edu.

Conclusions

1.) Multiple recent measurements have informed our understanding of the positron excess.

2.) Dark matter models appear unlikely. Stochastic acceleration and pulsar production appear reasonable.

3.) In particular, the large pair conversion efficiency of pulsars has gotten us halfway there.

4.) Electrons and positrons appear to escape pulsars efficiency. In this case they must produce the excess.

5.) HAWC observations offer the ability to observe the nearest pulsars, including systems missed by every other survey.

Extra Slides

Stochastic Acceleration

Propagation Model	ϕ_0	ϕ_1	a	b	c	d	χ^2_{tot}(per d.o.f.)
C	0.32	4.0	1.26	-0.125	-0.010	0.006	44.0 (0.86)
E	0.32	9.2	0.83	0.170	-0.046	0.007	59.6 (1.17)
F	0.32	15.6	0.94	0.055	-0.032	0.006	58.4 (1.15)

ISM model	$K_B^{\rm best}$	$K_B^{\rm 95\%upper}$	$K_B^{\rm 95\%lower}$	χ^2_{tot}	$\chi^2_{d.o.f.}$	$\Delta\chi^2_{tot}$(from back only)
C	6.1	7.6	4.6	34.0	0.68	10.0
E	10.4	12.4	8.1	39.9	0.80	19.7
F	7.4	8.9	5.7	37.5	0.75	20.9

Stochastic Acceleration

$$N_{CS}(E_{\rm kin}^{\rm ISM}) = a + b\ \ln\left(\frac{E_{\rm kin}^{\rm ISM}}{\rm GeV}\right) + c\left[\ln\left(\frac{E_{\rm kin}^{\rm ISM}}{\rm GeV}\right)\right]^2 + d\left[\ln\left(\frac{E_{\rm kin}^{\rm ISM}}{\rm GeV}\right)\right]^3.$$